Dear Editor and Reviewers,

We thank the three reviewers for their constructive comments and suggestions made in their reviews. In summary, we have made changes to every section, and re-drafted every figure to varying degrees. We believe the manuscript has been greatly improved through the review process.

Overall, we have shortened the introduction by removing the unecesary detailed description of the geochemistry and a number of sentences not relevant to the study.

We have added small description of Yerrida Basin, why it is complex, and how geophysical data can help better understand the complexity.

We have shortened the description and results around the structural interpretation leaving only the relevant parts. While it is important to describe, it took too much space in the original manuscript relative to its relevance.

We have significantly edited section 4, in particular, section 4.2, for brevity. We believe the generation of the hypothesis regarding the extents of the Killara Formation are clearer.

Significant changes to Section 5, with the introduction of a new figure (Figure 18) and explanation to early lava flows and intrusion in the partitioning of magmatism. This supports our hypothesis that the tectonic history to the Basin is more complex than currently thought.

We address specific comments below. Note that some comments have been addressed in the discussion phase of the review and can be accessed from our previous responses to the reviewers.

Sincerely,

Mark Lindsay
Sandra Occhipinti
Crystal LaFlamme
Alan Aitken
Lara Ramos

Perth, Australia
April 29, 2020

Reviewer comments and suggestions are highlighted in **bold**, our response are shown in normal font.

Note the most of the figure numbers cited below refer to the previous version of the manuscript. To aid easier assessment of this response the old and new figure numbering is shown below.

Table R1

Original Manuscript Figure number	Revision action	Revised manuscript Figure number	Notes
1		1	
2		2	
3		3	
4	**removed**		
5		4	
6		5	
7		6	
8	**removed**		
9		7	
10		8	
11		9	
12		10	
13		11	
14		12	
15		13	
16		14	
17		15	
18		16	
19		17	
		18	**new figure**

Reviewer 1

Specific comments - Manuscript

L120 "Implies there are no rocks between Juderina and Yelma - what happened to th rest of the Yerrida units"
There is an unconformity, and in this part of the region it is likely the basin didn't deepen enough for other units to form over the Juderina. Text updated.

L127
"Why?"
Because the possible synchronous deposition of the Juderina and Johnson Cairn formations with mafic volcanic rocks has generated further interest in the Yerrida Basin for potential VHMS mineralisation. Text added for clarification.

L194 "why mention these ? or put them in the strat column" and "Finlayson is nevermentioned again".
Agreed, 'member' level descriptions of the stratigraphy is not needed, so we have removed them from the manuscript.

L205 "not of interest to the reader".
We believe that the retention of geological plausibility is important during geophysical inversion, and is relevant to the geoscience community who we hope will read this manuscript. Thus the topological constraint is an important feature of the chosen method and is an important reason to justify our choice to use it. Given this justification is given in two sentences, we think these statements should remain. Section 4.2. A rewrite of this section will be performed to clarify which datasets were used in what capacity to produce the interpretation, but specifically describing those of relevance the to the inversion modelling. Thus the current emphasis on the magnetic data will be removed and clarified. Other suggestions around the correct citation of datasets and display in figures will be addressed.

L336 "how does it compare to your Noddy model?"
This kind of comparison is difficult to make. Noddy is kinematic modelling platform that takes essentially conceptual in-puts to produce a model. GM-SYS, while also driven at a higher level by concepts, is constrained with data. Thus the progression from Noddy to GM-SYS was performed to introduce the necessary detail to test the geological complexity that cannot be easily performed with a kinematic modelling platform. Noddy allows the introduction of simple flat and homogenous body of high density from which we can test the gravity response. GMS-SYS also allows this, but we can easily truncate, or fault, thin or expand the high-density body in an explicit manner. Nonetheless, the two methods produce consistent results. We have added text to refer readers to the previous section, and to better explain our reasoning behind using the two modelling methods to falsify (and the inverse action, support) the hypothesis regarding the Killara Formation and the moderate strength gravity anomaly.

L354: which are these? show in Fig 7a

We have revised figure 6 to show which faults have been included in the 3D model, and those that haven't.

L356: but not all units had measurements made on them
and
where did you get the unmeasured values from?
Reference to Telford et al. 1990 added to the results / petrophysics section (4.1)
Suggested edits from reviewers between L358 and L363 have been accomdated into a rewrite of this paragraph.

L369 "why not 2000m as in your Noddy model?"
2000m was an indicative thickness to produce an relative weak anomaly located over the Goodin Inlier. The purpose of the GM-SYS was to provide more precise while plausible estimates of thickness for the dense material that could then be input to 3D modelling. The result reported here shows that the Noddy thickness is likely more than needed. From this comment, we our logic in progressing from Noddy to GM-SYS to the 3D model needs to be better explained (see also our response to comments made in L336 above).

Note that we have rewritten the section 4.5 to better explain our reasoning for the assumed unit thickness. That the 2D section modelling combined with the thickness estimates of Pirajno and Occhipinti (2000) are consistent encouraged us to assume ~ 1000 m was plausible.

L398 "you must have allowed density changes as well to get high density units in areas where there were none to start with"
We didn't allow high density values to be placed anywhere in the model. This is why the 3D geological and topological constraints are important. The ranges of petrophysics forbid values being assigned to voxels in the location of these bodies during inversion. This means that high density values are only allowed in locations as specified by the 3D geological model. We have added text to clarify

L411 "not needed here - keep it in dedicated section"
Agreed, we have moved the consideration of dolomite to the discussion.

L421: "relationship to Juderina?"
Possibly – text added for clarity

L433: "space filler – remove"
Sentences rewritten.

L466 "why not in Juderina?"
The previous assumption was that the only mafic material in the Yerrida Basin could be attributed to the Killara Formation, or the late dykes. Thus we make comparison with the Killara to show the difference with the previous hypothesis, and the updated one provided by this study. A sentence has been added to clarify this point.

L497 (and further comments through this section) "So we are expecting DGDD to show Narracoota signatures?"

yes, based on the surface geology, but drilling shows that Windplain Group rocks underlie rocks contained within the Byrah Basin.
Sentence added to clarify why DGDD347 is an appropriate drillhole for this particular exercise.

L515 "this statement is quite a claim from only 2 holes one of which doesn't convincingly support your observations."
We appreciate this insight, however it's not clear why the reviewer believes one drillhole (not specified) doesn't support the observation. Section 5.5 Basin development A figure showing block diagram will be produced to support the interpretation in this section.

L534 and 536
Reference corrected and 1995 reference added.

Line 543: "doesn't the Juderina lie here too?"
True, however we argue that this could also be Killara Formation hosted in the upper units of the Mooloogool Group. We agree this is pure assumption, but so would it be that the host is Juderina. Given the prevalence of the Mooloogool units, we think it plausible for it to be Killara. Sentence added for clarity.

L553 "hence unlikely to be in regions 2 or 3 as suggested above - need to explain why no vents in regions 2 and 3 are seen in Fig 19"
Agreed, the assumptions described in Lines 544 to 548 is inconsistent with the sulphur isotopic results. While we have removed these lines, it doesn't change our overall interpretation. The result is a more consistent interpretation and we believe addresses most of the comments between lines 540 and 565.

L553 "hence unlikely to be in regions 2 or 3 as suggested above - need to explainwhy no vents in regions 2 and 3 are seen in Fig 19 "
The premise is that vents must bedistant to regions 2 and 3 given they are very likely sitting on Yilgarn Craton rocks giventhe structure shown in the 3D model. Thus, is vents were located in these regions,lavas erupted from these vents would have an Archean signature from interacting withYilgarn Craton rocks.L554 (and similar comment L555, L564) "are you suggesting the Goodin Fault is theedge of the craton?" No - we have evidence to suggest that, however the lack of anArchean signature suggests that there is an absence of Yilgarn Craton rocks. Wherethe boundary is located can be better addressed by further work.

L600 "and the origin of Killara mafics?"
This is described by Piranjo and Adamides(2000) and Occhipinti et al 2020.
We have added reasoning to the discussion to why we do not provide interpretation of the vents related to the Killara Formation (Lack of sulphur isotopic data). We direct readers to Pirajno and Occhipinti (2000) and Occhipinti et al. (2017) for those interested in this topic.

Reviewer 1

Specific comments – Figures

Merging of Fig. 1 (map/geophysics) and Fig. 2 (stratigraphy) –

We agreed that these two figures could be merged in the online discussion, however this has proven difficult. Geology in figure 1 is shown at the group level (e.g. Windplain and Mooloogool groups) while that in figure 2 is at the formation level. Merging these two would require figure 1 having more detail, which would make it hard to read, especially for an introductory figure, or would make figure 2 non-representative of input to the 3d model.

We have attempted to make the necessary link between the figures easier to achieve with appropriate annotations and explanation in the figure caption. We have also added annotation for major structures to help aid the descriptions in the Results and Discussion sections.

Figure 3 and Line 225 “If this is what you used, why not show it in Fig 7”,

We have shown this in Figure 3 so it can be seen without the interpretation overlay.

Figure 4. Grey scale colour mapping is preferred due to better contrast and colour-blind readers. The point of the figure is that features in the magnetic data are hardto spot once the irrelevant near surface anomalies are suppressed through upwardcontinuation.Figure 6. "why are there no density measurements for all the units that you havemag measurements for?" lack of outcrop and what outcrop there is weathered. Alimited selection of material was available from drill core due to company restrictionson destructive sampling.

Figure 7. "where is the colour Bouguer with the 1VD RTP which the authors said wasparticularly useful for the interp?"

This figure will be added (now Figure 3c)

"Where are the major faults that were used in the 3D modelling?"
These are now highlighted, and labels for the Goodin and Merrie Range Faults have been added.

We have also simplified the interpretation to make it easier to view (see also comments from Reviewer 3).

Figure 9. "could be merged with Fig 10" we tried this and the figure is quite large anddoesn’t fit into the manuscript while retaining legible labels.

Figure 11. "would be nice to see where the measurements that the authors madeplotted on this diagram to verify that the units matched the geological interp in part d".This is the purpose of Appendix Table A.1. Clarification will be added to the caption.Figure 16. The figure will be redrafted, along with comments supplied by the otherreviewers.Figure 17.

"green area represents?" Figure will be updated.Figure 19. Addressed in responses above to L553 and L554

Removed reference to the Finlayson and Bubble Well members due to irrelevance.

Figure 13 “never referenced - remove “ and “incorporate into fig 13” [note figure 13 is now figure 11]

We have kept this figure separate from figure 12 as it is discussed in some detail, and that figure 11 is quite large. It was difficult to incorporate this figure there. We have redrafted the figure made reference to part a in the text. The position of the density misfit in relation to the modelled geology is important to display for the purpose of discussion.

Figure 14:” very difficult to see what is going on here - would be better to have a 2D profile to clearly see the differences in depth”
Agreed and done

Figure 15 “green area represents?”

N-MORB – the label was obscured by data points. We have rectified this.

Figure 17 “what about the mafic seen in the Bryah basin? Isn't it more likely that this anomaly is due to them?”
And various questions line 540 to 565 about the discussion around this figure and model.

We have have generated a new figure (Figure 18 in the revised manuscript) that we hope better explains the model and how magmatic sources north of the Goodin Fault can deposit rock in the south. A paragraph has been added to the discussion to explain this part.

Reviewer 2

Specific comments

Is the petrophysical model on Figure 11 derived from the 3D inversion? If yes, please add a few words to be clear

Agreed. This has been done for clarity.

If all the figures have the same orientation, it is easier to compare them and see thedifference directly. Is there a special reason why Figures 12-14 show a different angleof view of 3D models?

We agree that some of these figures are a little difficult to view. We have made significant efforts to redraft and annotate Figs 12-14 (now Figs 10-12) to improve this. However, all these figures are viewed from the same orientation (isometrically from above and the SW), so we don't quite understand the point about different orientations. We do acknowledge that fig 16 (now fig 14) required additional work, and the changing orientations (above and below from the SW) does not assist the reader greatly. The other reviewers also made comments on this figure. We have reduced the number of views, and displayed results on a section (as per Reviewer 1's suggestion)

Reviewer 3

Specific comments - manuscript

"Line 16: I'm uncomfortable with the phrase "high amplitude density anomalies". Density is a parameter measured in g/cm3 (for example) and in my view, typically isn't referred to as having amplitudes (or wavelengths). It makes me think you're talking about a gravity anomaly - are you? At least for the purposes of clarity, I suggest the authors keep these two things distinct (density and gravity) since a gravity anomaly is caused by high density rocks. Please check throughout the MS."

We have replaced 'amplitude' with 'magnitude'.

Line 148: Is this 11km data helicopter land-based gravity? Like the mag, I think its worth specifying the years (or even decades) that these gravity stations were acquired. Elevation is a critical component to gravity data, and accurate elevations were much more difficult before GPS.
And
Line 149: I think its worth listing some of the processes that were applied to this gravity data in a sentence or 2. Tide, drift, theoretical correction formula used, gravity datum, FA correction and the density used for terrain/Bouguer corrections.

We have provided a reference to the dataset so the interested reader can access this information. Given the advice from reviewers 1 and 3 to shorten the manuscript, we believe this can help.

Line 179: A sentence or 2 here about what potential forward modelling actually is and how its done would help readers who aren't familiar with the technique. Ie – the objective is to iteratively adjust the geometries/rock properties to obtain a match between the observed and the calculated response etc.

The purpose of the exercise is described with the results (sections 4.3 – 4.5) to place the results of the method in context.

Line 216: I don't get why you've used gms/cm3. The SI symbol for grams is 'g'. I suggest you stick to this and leave it as 'g/cm3'. Please check throughout the MS.

This has been corrected

The suggested corrections and comments from Line 223 to 268 are no longer applicable due to deleted text addressing manuscript brevity, or have been addressed in the revision.

Line 275: 'density anomaly' do you mean gravity anomaly?
Yes, and corrected accordingly

Line 321: should be 'two scenarios were examined'
Corrected

Line 319: its not clear to me how the sensitivity of the dip direction of the Goodin Fault is relevant to the subcrop distribution of the Killara Fm.
Text added to clarify why this is important (also address in our initial responses to the reviewer).

Line 332: you seem to be referring to the geological section (line 328) and petrophysical model (line 332) interchangeably. Suggest you keep this consistent. Calling it a petrophysical model makes sense to me.
Agreed, this has been addressed.

Line 366: Do you mean 'figure 10a and b'??
No we are referring to the conceptual model results, the reference is correct.

Line 600: ok cool – I think its worth adding something here in the conclusions aboutprospectivity. Even if the spider diagrams for the mafics you've modelled show inclined profiles and therefore VMS-unprospective, I suggest its still a valuable conclusion
Agreed – sentence added to the conclusion.

Comments for Line 819 and 820: This figure and caption have been removed.

Line 860 "Caption is incomplete"
We have addressed this by adding the appropriate references.

Reviewer 3

Specific comments - Figures

Figure 2 - Can the colours on this figure be made consistent with those on figure 1? Or vice-versa?
The colours in figure 2 are consistent with the 3D model images, .while those in Figure 1 are colours for the group level as defined by the Geological Survey of Western Australia. See also response to Reviewer 1 on this issue. We'd prefer to keep the colours as they are, however we have added clarification to the caption.

I think it would help with clarity if ages were added to this strat column.- I realise the white spaces have been included to show that there are mafic intrusives, but this seems like an unusual way of visualising it to me in a strat column – I was expecting a blobby pluton shape of some sort to represent granites?

An intrusive-like shape has been added.

My first thought was that the white spaces were separating the groups until I read further and realised which formations belong where. I think it would help with understanding the regiona lgeological context if this figure was made more like a standard strat column with ages and graphics to represent overprinting (from granites for eg).

We agree with the suggestion and have made the necessary changes, however ages have not been added as they remain quite uncertain as there remains significant overlap to the ages of the Windplain and Mooloogool groups. This is mostly related to a lack of conclusive geochronology. As this figure is to serve a dual purpose to represent both the general stratigraphy and that which is input to the geological model, a 'traditional' space-time plot would require a new figure, and be contrary to the aims of making the manuscript more concise. See Occhipinti et al. 2017 for more details.

Figure 6. Adjust colour stretch, simplify interpretation and clarify different structures.
This figure has been redrafted to comply with suggestions made by Reviewers 1 and 3.

Figure 7.
Change 'gm/cm3' to 'g/cm3'
Ideally, the figure in 9a should have a colour bar showing magnitude of gravity values
Changes made
Reporting of Noddy model parameters
This initial exploration to the gravity response was performed on a conceptual basis, thus model parameters are not critical and detract from the purpose of the modelling. Strict adherence to geographic distances (eastings/northings) are important the for the 2D forward modelling and 3D modelling stages. While it would seem the x and y dimensions are shorter than they should be, the result would remain the same if they were strictly geographically constrained. We acknowledge that the vertical axis (i.e. the thickness of the model) is important for this exercise, thus we report it in the figure.

Figure 8 “Figure 10 - Is there any vertical exaggeration on these models? Or are they all 1:1? There is a vertical dimension, but no horizontal dimensions.”
See response to figure 7 regarding geographic coordinates

Figure 9
Comments and suggestions have been addressed – petrophysical labels added and caption editied.

Figure 10 “I’d prefer to see this figure as large as possible (full page width). There is alot of detail and its very difficult to see as is. This would enable you to label all the unitsinstead of just the main ones.”
Figure is now larger and all units labelled.

Figure 11 “Its difficult to see some of the details in this figure – particularly the distribution of mafics, and even more tricky in the circled areas of interest. Ideally it should be bigger, but I’m not quite sure how you manage this though. The only way I can thin of is to split the figure, but there is value in having them all together as I’m sure the author’s have surmised.”
This figure has been redrafted and made as large as possible to fit on one page with the caption. Additional annotations have been made for clarity and the caption edited accordingly.

Figure 13 Why are the cells here different colours? What do they mean? You saythey’re colour coded, but where can we see what the colours correspond to? I’m happywith these cells showing the increased distribution of mafics from what was previouslyinterpreted, but if there is no mention of what these colours are, why bother distinguish-ing them at all

We have added additional description to the text and caption to explain the colour represent the incremental addition of mafic bodies to the model to achieve a better fit to the observed gravity data. A legend has also been added to the figure.

Figure 16 Like the others, I think it would help if this figure was larger. Perhaps a fullpage figure with the 4 parts in one column? As is, its difficult to see the details.
We have made one view larger, but have provide a section view as suggested by reviewer for better display of the deeper mafic material near the northwestern edge of the Basin.

Mapping undercover: integrated geoscientific interpretation and 3D modelling of a Proterozoic basin.

Mark Lindsay[1], Sandra Occhipinti[1,2], Crystal Laflamme[1,3], Alan Aitken[1], Lara Ramos[1]

[1]The Centre for Exploration Targeting, School of Earth Sciences, The University of Western Australia, Crawley, Western Australia, 6009, Australia
[2]Mineral Resources, Commonwealth Science and Industry Research Organisation, Kensington, Western Australia, 6151, Australia
[3]Department of Geology and Geological Engineering, Laval University, Québec, G1V 0A6, Canada

Correspondence to: Mark D. Lindsay (mark.lindsay@uwa.edu.au; markdlindsay@gmail.com)

Abstract. Gravity and three-dimensional modelling combined with geochemical analysis ~~are used to~~ examine the subsurface within, and below the poorly exposed Paleoproterozoic Yerrida Basin in central Western Australia. Understanding the structure of a region is important as key features indicating past geodynamic processes and tectonic activity can be revealed. However, in stable, post-depositional tectonic settings only the younger sedimentary units tend to be widely exposed rendering direct observation of basement and intrusive rocks impossible. Geophysical imaging and modelling can reveal the structure of a region under cover. High ~~amplitude~~magnitude density anomalies around the basin cannot be reconciled with current geological knowledge in the case presented here. The ~~density~~ gravity anomalies infer an abundance of buried and high-density material ~~that is~~ not indicated by the surface geology. A hypothetical causative source for the high~~-~~ magnitude ~~density~~ gravity anomalies is ~~considered to be~~ mafic rocks that were intruded~~sion~~ and extruded~~sion of volcanic mafic rocks~~ during basin rifting ~~of the basin~~. The simplest and plausible stratigraphic attribution of these interpreted mafic rocks is to the Killara Formation within the Mooloogool Group. However, geochemistry reveals that the Killara Formation is not the only host to mafic rocks within the region. The ~~M~~mafic rocks present in the Juderina Formation ~~have~~ are largely ~~been~~ ignored in ~~previous~~ descriptions of Yerrida Basin magmatism and results indicate that they may be far more substantial than once thought. Sulphur isotopic data indicates no Archean signature to ~~the~~ these mafic rocks, a somewhat surprising result given the basement to the Basin is the Archean Yilgarn Craton. We propose ~~It is proposed t~~the source of mafic rocks ~~were sourced~~ are ~~from~~ vents located to the north along the Goodin Fault or under the Bryah sub-basin and Padbury Basins. The conclusion is that the formation of the Yerrida Basin involves a geodynamic history more complex than previously thought. ~~The utility to the approach described here is examined for application to cratonic sag basin environments.~~ This result highlights the value in geophysics and geochemistry to reveal complexity in the earlier geodynamic evolution of the basin that may be indiscernible from surface geology, but may have high importance for the tectonic development of the region and its mineral resources.

Formatted: Left

1 Introduction

The Yerrida Basin is a region comprised of Paleoproterozoic rocks located in the Capricorn region, central Western Australia. A series of sedimentation events and unconformities combined with a history of mafic magmatism and the presence of Archean greenstone belts and an inlier has produced complex geology that cannot be resolved from field studies alone. Thus, there is ~~presents~~ an opportunity to examine the covered geology~~ical architecture~~ of the Yerrida Basin with a range of geophysical techniques. This opportunity exists because multiple geophysical data are required to delineate anomalies that can be interpreted to be structure, rock bodies or both. That no individual physical field adequately reflects all the elements required to construct a meaningful model stems from the ambiguity of geophysical data (Nettleton, 1942;Fullagar et al., 2004). Different lithologies often share very similar characteristics for a single petrophysical attribute (igneous, metamorphic and sedimentary examples with magnetic susceptibility see Grant (1985) and Clark (1997); for density examples see Manger (1963)~~)~~. Differentiation between geological units is typically made with less ambiguity using multiple petrophysical attributes. For example Perrouty et al. (2012) and Lindsay et al. (2016) use magnetic susceptibility and density measurements for both structural interpretation and forward modelling to differentiate geological units. This scenario is not unique, and typically any geological investigation using geophysics requires at least two physical fields to reveal architectural elements with less ambiguity to the interpreter (Aitken and Betts, 2009;Blewett et al., 2010;Dufréchou et al., 2014;Lindsay et al., 2016;Perrouty et al., 2012). These examples show how increased interpretation confidence is provided by identifying co-located anomalies present in multiple datasets. The reasoning is that if an anomaly is present in multiple datasets it is less likely that: (i) the anomaly has not been introduced as an artefact during data processing or collection and (ii) it is significant enough that it influences each of the represented physical fields to produce a detectable anomaly.

An alternative and less sceptical viewpoint is to use multiple datasets to detect anomalies because some geology only has a detectable response in specific physical fields~~,~~ or with ~~certain~~ particular orientation. For example, gravity and magnetic data were used by Lindsay et al. (2017) and Kohanpour et al. (2018) to delineate structure from a region in the east Kimberley, northern Western Australia where magnetic data provided nearer-surface imaging of the crust, and gravity imaged the deeper structure. ~~Recognising that the density and magnetic properties that potential field data provide a restricted image of the crust, magnetotelluric data was included to include distribution of resistive properties which have been used to identify where fluid pathways and mineralised zones exist based the presence of conductive anomalies (Heinson et al., 2006;Dentith et al., 2018).~~ Brethes et al. (2018) use magnetic and electromagnetic data with field observations to perform interpretation of the Jameson Land Basin, Greenland, where at the smaller scale of their study, electromagnetic data imaged the surface and near-surface geology effectively and magnetic data imaged the deeper structure. ~~Greenland, and Kohanpour et al. (2018) use gravity and magnetic data in combination with numerical modelling to determine the existence and location of deep- and crustal-scale structures. Similar investigations to mafic magmatism have been effectively conducted using geophysical data and modelling.~~ Blaikie et al. (2014) use detailed gravity and magnetic surveys to compare the structure of maars and

diatremes in the Newer Volcanics Province (NVP, Victoria, Australia), and infer their eruptive histories. ~~At larger scales, Deng et al. (2017) developed a 3D image of lithospheric density in the Tarim block, central Asia, which is covered by 5-15 km of basin sedimentary rocks. A combination of seismic velocity, gravity topography and crustal thermal models permitted investigation of the history of deformation and related magmatism.~~

~~Geochemistry provides valuable insight to the interpretation process through rich characterisation of rocks with multiple elemental attributes. Fundamental differences between rocks and their composition can be identified, and in the case of magmatic rocks, the genesis and source of formation interpreted. Armit et al. (2014) use whole rock geochemistry to define characteristic rare earth element (REE) geochemical patterns to support their geophysical interpretation of rock types in their reconstruction of the northern Mount Painter Inlier. Perrouty et al. (2017) and Perrouty et al. (2018) use geophysical interpretation to identify dyke swarms in the Canadian Malartic, then use geochemistry to investigate metasomatic footprints for Au mineralisation.~~

Geological constraints~~is~~ are~~is~~ required to support geophysical interpretation and modelling. The inclusion of field- or core-collected data is arguably the best way to reduce geophysical and petrophysical ambiguity (Betts et al., 2003;Brethes et al., 2018;Perrouty et al., 2012). Husson et al. (2018) use geological measurements and interpretations in the form of a petrophysically attributed 3D geological model to constrain gravity inversion and locate karstified regions in the Languedoc area, southern France. Such regions, covered by large areas of regolith, transported cover or basin sedimentary rocks make opportunities to make relevant observations of the target rare. ~~Mineral explorers will require geophysics to explore effectively, even in areas with sufficient outcrop, as most exploration is now focused on targeting buried mineralisation (Müller and Groves, 2019). Thus~~Thus, a necessary reliance on petrophysical constraint ensues when geophysical interpretation and modelling become the only convenient methods to examine geologic structure.

This paper describes how different data sets were used to identify various parts of basin architecture through structural interpretation, geophysical forward modelling, 3D structural modelling, geophysical inversion and whole rock geochemistry. ~~Structure was interpreted through a combination of magnetic, electromagnetic (EM) and remotely sensed data and integrated with petrophysical measurements and geological field observations~~The initial hypotheses about basin structure were generated primarily from integrated interpretation of geological, gravity and magnetic datasets. Geophysical modelling was used ~~to further~~ expand understanding of architecture into three-dimensions. Geochemistry was used to determine whether the interpreted mafic bodies were likely to be the Killara Formation basalts, or different bodies that may be associated with the Juderina Formation. The results were ~~then considered~~used to determine whether and where the Yerrida Basin might be prospective for VMS mineralisation.

2 Yerrida Basin Geology

The Paleoproterozoic Yerrida Basin is located on the northern margin of the Archean Yilgarn Craton, within the southern part of the Capricorn Orogen (Figure 1~~Figure 1~~) and extends approximately 150 km from north to south, and 180 km from

Formatted: Font:

east to west. Other Paleoproterozoic basins are located at the margins to the Yerrida Basin: the Bryah sub-basin and Padbury Basin (north and west) and Earaheedy Basin (east). The Byrah sub-basin was recently found to be a sub-basin of the Yerrida Basin by Occhipinti et al. (2017). Archean rocks also bound the basin with the northern extent of the Wiluna Greenstone belt to the southeast, and Yilgarn Craton granite-gneiss to the east. The Archean Goodin Inlier sits within the Yerrida Basin. The Archean Marymia Inlier is located to the north and separated from the Yerrida Basin by part of Bryah Basin.

The stratigraphy of the Yerrida Basin, summarised in Figure 2~~Figure 2~~ and by Occhipinti et al. (2017), is comprised of underlying Archean basement of granite-greenstone rocks typical of the Yilgarn Craton. The Wiluna Greenstone Belt is located at the southeastern edge of and unconformably overlain by the Yerrida Basin. The Merrie Greenstone Belt is located at the eastern edge of the Basin and is unconformably overlain by Yerrida Basin and Earaheedy Basin rocks. The Goodin Inlier is an elliptical, roughly~~-~~ 30 x 45 km fragment of Archean granitic basement unconformably overlain by the Windplain Group, the basal units of the Yerrida Basin. Goodin Inlier rocks are heavily weathered, dominantly monzogranite and mostly undeformed except at its southwestern margin. East to southeasterly trending mafic dykes intrude the Goodin Inlier and are marked in places by sericitised feldspars produced by contact metamorphism (Adamides, 1998). The Marymia Inlier, also an Archean fragment, is located to the north and northeast of the Yerrida Basin and was likely reworked during the Paleoproterozoic (Bagas, 1999). Sedimentation patterns and development of the Yerrida Basin were likely influenced by both the Goodin and Marymia inliers and uplift early in basin development (Pirajno et al., 1998).

The development of the Yerrida Basin began with deposition of the c. 2200 Ma Windplain Group, followed by the 2180 to 1996 Ma Mooloogool and Bryah Groups (Occhipinti et al., 2017;Pirajno and Occhipinti, 2000). The rocks of the Windplain Group are representative of a shallow coastal and possible epicontinental setting (Occhipinti et al., 2017), while the rocks of the Bryah and Mooloogool Groups were deposited in relatively higher-energy and possible rift environments (Occhipinti et al., 2017;Pirajno and Adamides, 2000). Periods of magmatism are recorded primarily by the basaltic volcanic and intrusive rocks of the Killara and Narracoota Formations (Mooloogool and Bryah Groups, respectively), though other mafic intrusive and extrusive rocks are observed in other formations (Juderina and Karalundi Formations, Occhipinti et al., 2017) and as dykes (2200-2014 Ma) ~~–~~(Mueller, 2011;Occhipinti et al., 2017). The geodynamic evolution of the Yerrida Basin is interpreted as a pull-apart basin opening consistent with a trailing-edge marginal sag-basin (Pirajno and Occhipinti, 2000), progressing to a rift in the north (Bryah Sub-basin) (Occhipinti et al., 2017;Olierook et al., 2018). Continued extension resulted in the intrusion and extrusion of the Killara Formation tholeiitic basalts (Occhipinti et al., 1997). Basin development ceased with deposition of the Maraloou Formation (Mooloogool Group) shales and siltstones in a lacustrine environment (Pirajno and Adamides, 2000;Pirajno and Occhipinti, 2000;Occhipinti et al., 2017). The Mooloogool Group is unconformably overlain by the Yelma Formation (Tooloo Group) and is the basal unit of the Earaheedy Basin (Occhipinti et al., 2017).

2.1 Mineralisation Potential

The Yerrida Basin is host to epigenetic lead-carbonate and oxide mineralisation at the unconformable contact between the carbonate and sandstone rocks of the Juderina Formation and the overlying Yelma Formation (Pirajno and Occhipinti, 2000). The position of this unconformity in the southern part of the basin is likely due to it being exposed while sedimentation occurred further north. Potential for epithermal copper exists in the Thaduna Formation due to the presence of the Thaduna Copper Mine (Pirajno and Adamides, 2000). VHMS mineralisation is exhibited by the DeGrussa Cu-Au-Ag deposit (12.Mt @ 4.7% Cu and 1.8 g/t Au) and is associated with mafic volcanism at 2045 Ma (Hawke et al., 2015). While mineralisation is hosted in the Karalundi Formation of the Bryah Group, the synchronous deposition of the Juderina and Johnson Cairn formations (Occhipinti et al., 2017) has generated interest in the Yerrida Basin for VHMS mineralisation, especially along the northwestern margin and Goodin Fault~~.~~ given they likely influenced formation of the Basin.

3 ~~Methods and~~ Datasets and Methods

3.1 Rock Properties

Rock properties measured from samples collected from the study area provide an important constraint for any structural interpretation or modelling of geophysical data (Figure 1~~Figure 1~~). Samples were collected from outcrop and carefully assessed to be free of ~~contamination from~~ weathering and alteration, however it is noted that there is a higher risk of sample c~~e~~ontamination from surface outcrop than ~~t dd~~rillcore. Magnetic susceptibility and density properties help to guide reasonable discrimination of rock types from magnetic and gravity datasets during interpretation. ~~The rock properties are also used to constrain geophysical ambiguity during forward and inverse modelling in an attempt to ensure that some representation of the target geology is maintained.~~ The rock property data collected from the study area guided the classification of geological units in the structural interpretation and provided the basis of the susceptibility and density values used in forward modelling.

3.2 Potential Field Data

Magnetic data (Figure 3~~Figure 3~~a) was obtained from the Geological Survey of Western Australia in grid form with an 80 m cell size that had been differentially reduced to the pole (dRTP) (Brett, 2013). The resulting dRTP grid is a mosaic of government-funded aeromagnetic surveys with line-spacing between 200 m and 400 m, and flown at heights between 80 m and 90 m depending on the individual survey. Various transforms and filters were applied to the dRTP grid to subdue or enhance particular features and included tilt, vertical and horizontal derivatives, analytic signal, upward continuation and dynamic range compression (DRC - see Kovesi et al., 2012 for details).

Bouguer gravity data (Figure 3~~Figure 3~~b) were obtained from the Australian National Gravity Database maintained by Geoscience Australia and have been corrected for terrain and spherical-cap effects (Brett, 2017). Older data from the eastern part of the Capricorn Orogen preserve topographic effects as only the most recently acquired surveys are terrain-corrected. Most gravity data have a station spacing of between two and four km, however in areas of more sparse coverage spacing can be up to 11 km. A grid was interpolated using a minimum curvature algorithm (Briggs, 1974) and used for interpretation and modelling. The gravity grid and variations were produced with a cell size of one km to provide the necessary detail and coverage.

3.3 Structural Interpretation

Integrated geological interpretation was conducted using primarily geological, gravity, magnetic and digital elevation model data. It was expected that ~~A~~aeromagnetic data ~~was used to~~would be effective to ~~-~~interpret the upper crust to determine the smaller-scale structural architecture ~~with methods~~ as demonstrated by Aitken and Betts (2008), Betts et al. (2007), Gunn (1997) and Lindsay et al. (2017). However, ~~.. Magnetic data~~magnetic data was not as useful in comparison to these cited studies ~~was difficult for extracting geological content~~ for the following three reasons:~~.~~ (1) ~~T~~the basin sedimentary rocks do not display enough magnetic susceptibility contrast to allow discrimination of structure; (2) the basin architecture is mostly flat-lying, thus most rock boundaries (and thus potential locations of high petrophysical contrast) were parallel to the plane of view used during interpretation and; (3) magnetic regolith and stream sediments obscure the underlying structure. Typical signal processing

~~Low-pass and upward continuation processing was used to remove the shorter wavelengths in the magnetic signal in order to lessen the obscuring effect associated with these magnetic cover units. Upward continuation also removed shorter wavelengths that may have been associated with the bedrock geology, making detailed near-surface structural interpretation more difficult.~~

~~The following~~ filters proved the most useful for magnetic data in different areas on the Basin: upward-continuation (to remove shorter wavelength and near-surface responses), the first vertical derivative (1VD); auto-gain control (AGC); tilt-derivative (TDR) and dynamic range compression (DRC) processing of Kovesi (2012). The combination of magnetic data with gravity proved the most helpful, with '~~b~~B~~l~~lend~~ed~~ing' grids facilitated better ~~resolution~~ imaging of structure, where two grids are overlain, and one is made semi-transparent. In particular, combination of ~~This practice was particularly useful with the magnetic data.~~ Bouguer gravity data and the 1VD of the magnetic RTP ~~its 1VD~~ was used ~~to identify larger structure, and~~ to provide additional insight to regions where magnetic susceptibility contrast was low (Almalki et al., 2015;Fairhead, 1976;Hildenbrand et al., 2000) (Figure 3c).

Field-based geological information was obtained from "WAROX", the Geological Survey of Western Australia (GSWA) rock observation database (Geological Survey of Western Australia, 2018)~~[44]~~ and used to locate some structures, but was principally employed to understand geometry and orientation of interpreted structures. WAROX data was invaluable for generating a 3D understanding.

3.4 Two-Dimensional Joint Magnetic and Gravity Forward Modelling

The map interpretation was supported by geophysical forward modelling a section crossing the northwestern part of the Yerrida Basin (Figure 3~~Figure 3~~a and b) to provide a platform for hypothesis testing and thus an understanding of the basin architecture at depth. The section transects the northwestern edge of the Yerrida Basin, the Goodin Inlier and part of the central part of the Basin. The structure and geology of the surface and upper crust was constrained predominantly by geological observations taken from WAROX and GSWA 1:100 000 (Doolgunna, Mooloogool, Thaduna) and 1:250 000 (Glengarry, Peak Hill) scale maps (Appendix 1) and our own fieldwork. The petrophysical model generated by forward modelling was constrained with density and magnetic susceptibility data that supported the subsequent geological interpretation. Forward calculation of the geophysical response was undertaken using the GM-SYS application in Geosoft Oasis Montaj® (https://www.geosoft.com/products/oasis-montaj) software following the methods of Talwani et al. (1959).

~~The purpose of forward modelling with this method is hypothesis testing so possible geological scenarios are tested against the observed geophysical data. Scenarios were proposed that explored different dip directions of the Goodin Fault, and the configuration of high density bodies (single or multiple superposed bodies) along the section. The model with the lowest misfit that also plausibly corresponds to the geology is presented in the results section.~~

3.5 ~~3D~~ Three-Dimensional Modelling and Geophysical Inversion of Gravity

3D modelling was performed using Intrepid Geophysics Geomodeller© (Calcagno et al., 2008). The purpose of producing a model was two-fold: (1) to better understand the 3D architecture of the basin and; (2) test the modelled architecture against the observed regional geophysical response across the entire basin. Geophysical modelling techniques were both 3D forward modelling (Talwani and Heirtzler, 1964;Talwani et al., 1959) and geophysical inversion (Guillen et al., 2008). Geomodeller software allows the stratigraphy to be defined as a topological constraint with interpreted structure deformation assigned to each stratigraphic unit, so that deformation timing can be established and only geological units of equivalent age or older are affected. As with all 3D modelling packages, some upscaling of data needs to be performed (Lindsay et al., 2012), so only the larger and more significant structures were included. This is because of limitations in the algorithms these packages use in reproducing complex geometries typically encountered in the natural world (Jessell et al., 2014). Stratigraphy was treated similarly, and the modelled units were limited to formations~~. For example, the Finlayson and Bubble Well members were not modelled individually, but represented by the parent Juderina Formation~~. Likewise, the 3D modelling algorithm provided by Geomodeller does not allow for joint modelling of more complex geological relationships, such as equivalent facies nor intercalated formations (for example, the Doolgunna and Thaduna formations) (de Kemp et al., 2017). Simplifications are thus required with all formations being represented as discrete units, though still belonging to the same group. The stratigraphic input data are summarised in Figure 2~~Figure 2~~.

Geophysical inversion was performed using the 'total litho-inversion' method of Guillen et al. (2008), a stochastic process which obtains a 3D probabilistic description of geological objects while constrained by the available data: geological

boundaries (our interpretation), petrophysics (density) and the observed geophysical field (the gravity grid). A range of model geometries and rock property values are tested and returns a model and a probability distribution over model space which addresses issues surrounding deterministic inversion methods of non-uniqueness and attempting to identify the 'best' or 'most probable' model (Tarantola, 2006). The input to inversion is the geological model with petrophysical properties assigned to each formation. Inversion can result in some violations of model topology, where implausible stratigraphic relationships are recovered as they provide a less costly mathematical solution. This method allows application of constraints ~~to applied~~ to ensure that model topology (i.e. the stratigraphy - Figure 2~~Figure 2~~) was not violated and that recovered lithologies remain in the correct stratigraphic ~~correct~~ order.

3.6 Geochemistry

Ultramafic and mafic rock samples obtained from the Yerrida Basin were analysed for major and trace element geochemistry at the commercial ALS laboratory, Perth~~hh~~. Further details (data tables and methods) are provided in the supplementary materials of Olierook et al. (2018).

4 Results

4.1 Petrophysics

Table 1 shows the measured values of both magnetic susceptibility (in SI×10^{-3} units) and density (~~gms~~g/cm^3) from rocks representative of the Yerrida Basin stratigraphy and input for forward and inverse geophysical modelling. Sample locations are shown in Figure 1~~Figure 1~~. The magnetic susceptibility values show very little variation between rock units. ~~This,~~This combined with the magnitude of error that envelops the range of susceptibility values across the measured rock unit, means that accurately differentiating geological bodies with magnetic data in this location is unlikely. Density petrophysics do show greater variability between rock units with less error meaning that gravity data may be more useful than magnetic data to differentiate geological bodies during forward modelling, even at a lower resolution when compared to the magnetics data. Figure 4~~Figure 5~~ shows histogram representation for each unit and Figure 5~~Figure 6~~ shows the same for density. Not all geological rock units used in the geophysical and 3D modelled have measurements obtained from field-collected samples. Generic values taken the corresponding lithology from Telford et al. (1990) were used when otherwise unavailable.

Formatted: Font: Not Bold

Formatted: Font: Not Bold

Field Code Changed

Field Code Changed

4.2 Structural Interpretation

~~Initial~~ The structural interpretation (Figure 6~~Figure 7~~a) was started by using ~~completed using~~ gravity data to develop a basin-scale structural framework.~~at the basin scale. The most useful combination of images at this stage was a blend of the Bouguer anomaly in colour and the 1VD of the RTP magnetics.~~ Some obvious features are the greenstone belts (Wiluna in the south, and Merrie in the east) characterised by a high magnitude gravity anomaly (Figure 6~~Figure 7~~b), and north-northwest trending strong and linear magnetic anomalies, as shown in the RTP/1VD blended magnetic image (Figure

6~~Figure 7~~c). The Goodin Inlier (Figure 6~~Figure 7~~a) is particularly obvious due to its low gravity signature in contrast to moderate signature surrounding it (Figure 6~~Figure 7~~b). The higher magnitude, moderate gravity signature also appears to be quite extensive, and is observed, in some places, to extend to the basin extents (Figure 3~~Figure 3~~b – white line). This suggests the moderate magnitude anomaly is in response to Yerrida Basin rocks, rather than the lower magnitude response basement, as exemplified by the Goodin Inlier. The Wiluna Greenstone belt is interpreted to extend under the southern edge of the Yerrida Basin (interpreted boundaries indicated by the yellow line in Figure 6~~Figure 7~~b) as its characteristic signature extends almost as far north as latitude 26° south, and dominates the gravity response of the southeastern corner of the basin.

More detailed structural interpretation at 1:100 000 scale relied upon existing GSWA geological maps, the WAROX (GSWA field observation database), magnetic data, orthophotos, digital elevation models, Landsat 8 and ASTER data provided as CSIRO Geoscience products (Cudahy et al., 2008). Gravity data was used where resolution allowed structure to be interpreted. ~~Two stages of interpretation were conducted. First, linear and planar geologic structure such as faults, fractures, dykes and folding was interpreted by using a combination of the available data, then lithology was interpreted (Figure 7a). The two stages were not conducted in isolation, as each stage needed to be consistent with the other to maintain basic geological principles and rules, and thus plausibility.~~

In both parts of the interpretation, magnetic data proved to be less useful here than other data. The magnetic grids show very little contrast in the Yerrida Basin rocks (Figure 6~~Figure 7~~c), and this is supported by the magnetic susceptibility results shown in Figure 4~~Figure 5~~. Some of the interpreted faults are supported by field mapping, the geological maps, the DEM and our own field validation (Figure 1~~Figure 1~~ – note site locations). ~~Some faults were interpreted from anomalies using a combination of magnetic data processed using dynamic range compression (Kovesi, 2012), auto gain control and the 1VD. Nonetheless, in many cases the suspected location and presence of faults needed to be supported with remotely sensed data, with the DEM being particularly useful. As such, deeper faults with no surface expression may not have been captured in this interpretation, aside from those interpreted from gravity data.~~

~~Lithological interpretation relied more heavily on datasets other than potential fields. Typically, lithologies can be discriminated successfully by observing textural differences in magnetic data, with variations in amplitude, frequency and orientation given particular lithologies as characteristic signature (Aitken and Betts, 2009;Betts et al., 2004;Lindsay et al., 2016;Perrouty et al., 2012) . The RTP data shows near-surface anomalies interpreted to be surface processes such as stream and channel sediments and magnetic regolith (for example Fe and/or Mg-rich lag) (Figure 4 – circled in red). Upward continuation was used to filter out these effects by attenuating the shortest wavelengths in the data.~~

~~Remotely sensed data was more useful for interpretation, but used with caution as regolith in the Yerrida Basin is widespread and covered any basin rocks that could be interpreted from satellite data. The widespread extent of regolith was confirmed by our own field observations. Airborne electromagnetic (AEM) data was helpful here, and showed that in some cases bedrock geological could be inferred from what is interpreted to be in-situ regolith (Figure 8a).~~

The interpretation (Figure 6~~Figure 7~~a) shows an overall E-W, or WNW-ESE orientation of structure in the west and centre of the basin. Structure in the east and southern part of the basin show an orientation of mainly NNW-SSE, similar to the

Field Code Changed

Formatted: Font: Not Bold

orientation of the underlying Archean greenstone belt and suggests inherited structure from the basement into the basin. The lithological interpretation differs little from existing 1:100 000k and 1:250 000k GSWA maps, and shows that the Juderina Formation forms the base to much of, if not all, the Basin. ~~The Johnson Cairn Formation is less extensive at the surface and is restricted to the western parts of the Basin. Some outcrop in the east suggests the Johnson Cairn may extend under the overlying Mooloogool Group rocks from west to east. A lack of outcrop of interpreted Johnson Cairn Formation in the south suggests it does not extend far to the south, if at all.~~

The most intriguing part of the interpretation relates to the Mooloogool Group rocks, which are interpreted to be located in the central, west, east and northern parts of the Basin, with the youngest rocks of the Maraloou Formation being the southern-most. The tholeiitic basalts of the Killara Formation are most extensive in the east, with some outcrop in the central, northern and western parts. This was unexpected, and thus interesting, as basaltic rocks are usually the densest rocks in a field area and contribute to stronger gravity anomalies. ~~This was unexpected, as t~~The initial interpretation of the gravity data showed a moderate magnitude anomaly to be extensive everywhere in the basin (Figure 6~~Figure 7~~b) which ~~, and~~ was initially assumed ~~to be the~~as Killara Formation due to the presence of higher density ~~of~~ mafic rocks relative to the lower density~~basin~~ sedimentary rocks. Thus, the initial interpretation of the Killara Formation shown in Figure 6~~Figure 7~~a may not adequately represent its true extent. If the higher magnitude ~~density~~ gravity anomaly observed throughout the Yerrida Basin is caused by the Killara Formation, then the extent of this formation ~~needs to~~may be far more extensive. The next sections describe how forward modelling and inversion ~~that~~ attempt to falsify th~~is~~e hypothesis that the Killara Formation is far more extensive than initially thought.~~.~~

4.3 Forward Modelling

Petrophysically constrained forward modelling of geophysical data was conducted to test the hypothesis that the Killara Formation is more extensive undercover than was shown through interpretation. Three stages of forward modelling were conducted: (1) a 3D conceptual study to validate our primary assumptions; (2) 2D section modelling of geophysical data with geological constraints and; (3) forward modelling of a 3D geological model.

4.4 Conceptual Modelling: Noddy

'Noddy' is a kinematic modelling package that allows input of geological events and stratigraphy to generate a 3D model of the resulting architecture (Jessell, 1981;Jessell and Valenta, 1996). A useful part of Noddy is being able to generate the potential field forward response of the model. By assigning petrophysical values to each stratigraphic layer in the model, a representative grid of the model can be generated (the 'calculated response') and compared to that provided by the geophysical survey (the 'observed response' – Figure 7~~Figure 9~~a and b). Figure 7~~Figure 9~~c shows the basement configuration of the conceptual model with the assigned petrophysical attributes. The Yerrida Basin (not shown in Figure 7~~Figure 9~~c) is thus ~~thus~~ assumed to have Archean basement, with the exposed Goodin Inlier forming a dome.

Three geological scenarios were explored (Figure 8~~Figure 10~~). The first simulates that no Killara Formation is present to explore what the geophysical response would be if there was very little, or no high-density material in the Basin (Figure 8~~Figure 10~~a). The second simulates a 500 m thick layer of high-density material representing the Killara Formation in stratigraphic position (Figure 2~~Figure 2~~) between the Maraloou and Doolgunna formations (Figure 8~~Figure 10~~b). The third simulates 2000 m of high-density material (Killara Formation) in stratigraphic position (Figure 8~~Figure 10~~c). The resulting gravity grids are shown in greyscale with the corresponding model, and profiles (A – A') sampled from the gravity grids.

Having no dense material in the basin (Figure 8~~Figure 10~~a) clearly does not recreate the observed gravity response with the Goodin Inlier producing a gravity high, rather than the low as shown in the observed response (Figure 7~~Figure 9~~b). Adding 500 m of dense material (Figure 8~~Figure 10~~b) produces a marginally closer fit to the observed response, but the Goodin Inlier still produces a gravity high, though with a lower difference (8.7 mGal) than in the previous example (15.7 mGal). Adding 2000 m of dense material does produce a response that shows the Goodin Inlier to produce a gravity low, and somewhat similar to the observed response. However, this calls for the Killara Formation to be consistently 2000 m thick, which is twice as much as the 1000 m formation thickness estimated from previous work (Pirajno and Adamides, 2000).

The results from conceptual modelling with Noddy support the hypothesis that a significant amount of dense material in the basin can produce the gravity response seen in the observed data. However, the reality is almost certainly more complex than a single, horizontal and lithologically homogenous layer. The dense material is likely to be a combination of widespread Killara Formation and sills or possibly intrusions produced through related magmatism.

4.5 Testing Intrusive Scenarios with 2D geophysical forward modelling

Geosoft® GM-SYS is a forward modelling platform that allows easy exploration of geologically complex scenarios (Talwani and Heirtzler, 1964;Talwani et al., 1959). A profile was selected that extended from the northern edge of the basin to the southeast, across the Goodin Fault, the Goodin Inlier and into the centre of the basin (Figure 3~~Figure 3~~) and in similar location to the profiles produced in Noddy (Figure 7~~Figure 9~~a). The same hypothesis is being tested: whether the dense material, possibly the Killara Formation and its intrusive components can account for the gravitational response in this region, however this form of forward modelling allows for more complex geometries to be tested manually.

A selection of plausible models were generated in accord with the geologic history of the region. The main questions were:

(1) how sensitive is the gravity response to the dip-direction of the Goodin Fault? This was tested by changing the dip direction from the northwest, to sub-vertical, and to the southeast. The dip-direction of the Goodin Fault has implications for basin development, with the direction inferring which side of the fault forms the half-graben shoulder during sedimentation.

(2) what configuration of high- -density bodies are required?- Two scenarios were examined, one where the high-density bodies were assumed to be extrusive mafic lavas associated with the Killara Formation, thus no intrusive component. The other was that multiple superposed bodies were possible, so assuming both intrusive and extrusive modes of magmatism.

Five scenarios were generated from these assumptions. Figure 9~~Figure 11~~ shows the ~~model which~~model that is ~~the~~ most consistent with the geological interpretation (Figure 6~~Figure 7~~), geological observation (Table A1) and the potential field geophysical data (Figure 3~~Figure 3~~). Figure 9~~Figure 11~~a and b show both the magnetic and gravity (respectively) observed response (dots) and the calculated response (line). The calculated response is produced from the ~~geological~~ petrophysical model~~section~~ (Figure 9~~Figure 11~~c), where petrophysical values are assigned according to values measured from the field. The geological section was constructed using geological observations taken from GSWA maps and WAROX (Appendix 1), and interpreted using the ~~integrated into the~~ petrophysical model so that existing structural relationships are maintained, and general geological reasoning is not violated.

The model fits well to both the magnetic and gravity data. Geological interpretation (Figure 9~~Figure 11~~d) of the petrophysical model (Figure 9~~Figure 11~~c) shows that the Killara Formation ~~has been successfully~~can be modelled as a set of faulted sills and is broadly consistent with the conceptual modelling results shown in the previous section. Importantly, the 2D section forward modelling shows that these sills need only be 1000 m thick. The combination of modelling results ~~s. This~~ support~~s~~ the hypothesis that the Killara Formation may be the source of the moderately high gravity anomaly throughout the Yerrida Basin. This interpretation of sills and intrusions is thus still consistent with that of Pirajno and Adamides (2000) and their thickness estimates.

At the northwestern end of the section (left-hand side of Figure 9~~Figure 11~~d), the boundary between the Yerrida Basin rocks (Doolgunna and Juderina formations) and the Byrah Basin rocks (Karalundi Formation) has a distinctive signature, especially in the magnetic data (Figure 9~~Figure 11~~a). The geological model shows a very steep dip to the northwest (or left-hand side of the section) and a possible downward throw as indicated by the footwall Yilgarn Craton modelled on the Yerrida Basin side of the boundary. The Goodin Fault has been suggested to be at this location, and this model shows it to be a normal, northwest dipping fault, in contrast to the northwest dipping thrust structure reported by Pirajno and Adamides (2000) but consistent with the interpretation of Occhipinti et al. (2017). The analysis presented here is certainly not conclusive, and the presence of the Goodin Fault is still under question, as are its characteristics.

4.6 3D Model

The hypothesis of mafic rocks attributed to the Killara Formation are the causative source of the gravity anomaly throughout the basin now appears feasible. Hypothesis testing on simple models and a section around the Goodin Inlier provide some

support, but whether this relationship is consistent for the entire basin also needs to be tested. Modelling was expanded to include the entire basin in 3D to achieve these aims.

A 3D model was constructed using Geomodeller, an implicit modelling platform that allows models to be constrained by known stratigraphy, fault relationships and geological observations (Calcagno et al., 2008). Geomodeller also offers geophysical modelling tools, including forward modelling and inversion (Guillen et al., 2008), which operate directly on the 3D geological model.

Data input to the model was gathered from the stratigraphy (Figure 2~~Figure 2~~) and structural interpretation (Figure 6~~Figure 7~~a, Figure 9~~Figure 11~~d). However, only the larger faults were retained for 3D modelling, as the smaller, more insignificant faults degrade performance of the modelling engine without providing a commensurate increase in geological understanding to this study. Each geological unit constructed in the 3D model has petrophysical values (Figure 4~~Figure 5~~, Figure 5~~Figure 6~~) assigned to allow a forward response to be calculated.

The 3D model contains what were considered ~~to be~~ important components to produce a representative geophysical response: the Goodin Inlier; Archean basement; Yerrida Basin sedimentary and magmatic rocks; the Wiluna and Merrie greenstone belts and various faults, including the north-northwest-ward extension of the Ida Fault (Figure 10~~Figure 12~~).

The Bryah-Padbury basin, located in the northwestern corner of the model volume, is ~~It is imp~~not included in the model. This region is complex both geologically and geophysically in its own right, deserving of a dedicated study, and thus not the focus of this work. ~~ortant to note the northwestern corner of the model, where the Bryah-Padbury basin would be, is not included in the modelling.~~ Likewise, the structure of the surrounding Archean greenstones is complex and is addressed by ~~The focus of this study is on the Proterozoic basin rocks rather than the Archean basement as~~ Giraud et al. (2019) and Giraud et al. (2020) ~~described~~ in a comprehensive analysis of the underlying greenstone belts using sophisticated inversion techniques constrained by uncertainty estimation.

4.7 3D Forward Modelling and Inversion.

3D forward modelling was performed to investigate the density structure of the Yerrida Basin. Initial attempts at modelling the gravity produced similar results to those shown in the conceptual stage (Figure 8~~Figure 10~~b and b). Including the Killara Formation as a thin unit showed that this had almost no effect in producing a gravitational anomaly (Figure 8~~Figure 10~~b). Learning from this result guided the construction of the 3D geological model to include a more substantial component to the Killara Formation. The modelled intrusive bodies were quite thick (=>1000m) and extensive but were still not sufficient to replicate the observed signal. Evidentially an additional source of high-density material needed to be considered.

4.8 Juderina Formation and a Substantial Mafic Component.

Drill core from a range of diamond-drilled boreholes (THD1, DGDD347, DGDD020, DGDD278, DGDD279, DGDD281, DGDD319, DGDD320, DGDD404, DGDD406 and THDD 226) reveal that the Juderina Formation also contains mafic sills, either as finer-grained basaltic, or micro-gabbroic rocks at depth. This observation is particular to the Juderina Formation,

Formatted: Font: Not Bold

Formatted: Font: Not Bold

Field Code Changed

Field Code Changed

and not the overlying Johnson Cairn, Thaduna, Doolgunna and Maraloou formations. Reasoning suggests that the mafic component of the Juderina Formation was intruded during or soon after deposition of the clastic and carbonate component of the formation, and was thus restricted to just this formation. Another option is that the mafic component to the Juderina Formation is related to the intrusive parts of the Killara, Karalundi or Narracoota formations, however if this was true, formations underlying the extrusive Killara Formation component (Johnson Cairn, Thaduna and Doolgunna formations) should also contain some proportion of mafic intrusive rocks, which (to our knowledge) they do not. Thus, adding higher density bodies proximal to or within the Juderina Formation is a reasonable means to reproduce the anomalous gravity signature.

Geophysical inversion provides a means to test the hypothesis that higher density rocks can explain the anomalous density signature. An incremental approach was taken, similar to that with the simplified conceptual models (Figure 8~~Figure 10~~) ~~was taken~~ to ensure that multiple scenarios ~~are~~ were considered while simultaneously performing sensitivity analysis. The following scenarios were tested:

~~1.~~ Scenario 1: No additional high density intrusions are modelled – only the Killara Formation rocks are high density (>3.0 gm/cm^3)

~~2.~~ Scenario 2: A moderate increase in the volume of ~~high density~~high-density intrusions in locations suggested by the section-based forward model (Figure 9~~Figure 11~~)

~~3.~~ Scenario 3: A large increase in the volume of high-density intrusions, as guided by the location of high-density anomalies in the observed gravity data (Figure 3~~Figure 3~~b).

Inversion was conducted by discretising the geological model into cells of 2000m x 2000m x 500 m (x, y and depth axes respectively). The maximum number of iterations was set to 1M but convergence was reached ~~was exceeded~~ before this was exceeded~~convergence was achieved~~. The 'success' of the inversion was judged on global statistics (RMS misfit) and locally, by investigating how inversion produced the necessary density structure to reproduce the observed gravity field at specific locations.

Each inversion was executed to allow the contacts of the Juderina Formation, intrusive bodies and the Archean greenstone units to move if required by the inversion. All other units ~~were left~~ remained 'fixed' and their contacts were unable to move. Regions hosting high-density rock bodies were added to the model in plausible locations according to where the gravity response is stronger (e.g. Figure 11c and Figure 11d). These constraints reflect our knowledge of which rock units contain high-density rocks, and whether changing the geometry or petrophysical properties of these particular rocks can explain the density structure of the Yerrida Basin.

All scenarios were modelled via inversion successfully ~~inverted.~~ ~~and produced a~~ A root-mean-square (RMS) misfit of approximately 4 mGal from an initial misfit of over 20 mGal, with the final misfit values ((Figure 11~~Figure 13~~) and

Formatted: Indent: Left: 1.75 cm, No bullets or numbering

Field Code Changed

convergence curves almost identical. While a 'successful' inversion and corresponding reduction of RMS misfit by 80% is satisfactory, the almost identical convergence curves and final RMS values alone are inadequate ~~as~~ indicators of geological plausibility. Deeper geological analysis of the resulting model is needed. ~~Results are shown in Figure 13.~~ Figure 11~~The upper panel of part (a)~~ shows the geological model at left, the ~~middle panel shows the~~ observed gravity data at ~~-~~centre ~~that was input~~ and the ~~the lower panel shows the~~ prior model extents of the Wiluna and Merrie greenstone belts ('W' and 'M' respectively~~) at right)~~. The left-hand panels of Figure 11 ~~P~~parts (b), (c) and (d) ~~top panels~~ show the ~~geological~~ prior geological model used for input (scenarios 1, 2 and 3 respectively). ~~with o~~Only the included mafic intrusions are displayed ~~for~~ for easier ~~ease of~~ visualisation. The ~~middle~~ centre panels of Figure 11~~(~~b~~) d, (c) and (d)~~ show the gravity ~~field~~ response calculated from the inverted model. The right-hand panels of Figure 11b-d show the 3D inverted model filtered to only display cells with ~~A~~ minimum density threshold of 2.9 g~~m~~/cm^3. This density value was ~~was~~ chosen so that only ~~as only~~ high-density, and thus most likely only mafic rocks. ~~are generally expected to show density higher than this~~ are visible over those that may be dolomitised (Telford et al., 1990). Consideration of dolomitisation as high-density material is presented in the Discussion.~~Another plausible possible source of higher density material in this region is dolomite, however these are unlikely to have densities >2.9 gm/cm³ (Telford et al., 1990). Thus the lower panels of Figure 13 shows the distribution of locations determined by the inversion to be > 2.9 gm/cm³ density and possible mafic bodies. A discussion whether dolomite or basalt is more plausible is conducted in the next section.~~

The ~~middle~~ centre panels of Figure 11~~Figure 13~~ ~~highlight~~ have circles that indicating two ~~regions~~ locations that ~~are~~ were investigated in more detail: '1' – in the west; and '2', in the centre of the Yerrida Basin.

Region 1: The observed gravity data shows a high magnitude anomaly in Region 1. The ~~lower~~ right-hand panels in Figure 11~~Figure 13~~b-d show that the inversion requires dense material >2.9 gm/cm^3 to be placed ~~here~~ in the circled locations to~~to~~ account for the anomaly in the observed data (Figure 11~~Figure 13~~a ~~middle~~ centre panel)~~, regardless of the geological prior model used for input.~~. Scenarios 1 and 2 do not have mafic bodies modelled in this location (see ~~upper~~ left-hand panels), so the model requires rocks within the Juderina Formation with ~~exhibit~~ densities ~~at~~ >2.9 gm/cm^3 to better reproduce the observed response ~~in these inversion results from these scenarios~~. Subsequently, ~~S~~Sceenario 3 includes a mafic body in this location, possibly also hosted by the Juderina Formation (Figure 11~~Figure 13~~d – ~~top~~ left panel), and the inversion includes higher density material in this location as well, but more laterally extensive than in scenarios 1 and 2.

Region 2: The observed gravity data shows a higher ~~amplitude~~magnitude gravity anomaly in this location (Figure 11~~Figure 13~~a – ~~middle~~ centre panel). To the east, the deeper presence of the northern extension of the mafic component of the Wiluna Greenstone Belt (WGB) is interpreted to be the causative body of the higher magnitude gravity ~~values~~ response (Figure 11~~Figure 13~~a ~~bottom~~ centre – 'W'). The western edge of ~~the high amplitude~~this region also displays a high ~~amplitude~~magnitude anomaly, though of lesser magnitude than the WGB (Figure 11~~Figure 13~~a-d - white box). Scenarios 1 and 2 show that this part of the model is not adequately resolved through inversion. ~~, while~~ Scenario 3 shows some improvement in the region outlined by the white box, though not enough to explain the southerly portion of the anomaly. A

zoomed comparison is shown in ~~middle~~ centre panel inset of Figure 11~~Figure 13~~a (observed field) and Figure 11~~Figure 13~~d (inverted model calculated gravity response). An~~:~~ ~~the~~ asterisk in Figure 11d (centre) indicates where additional higher density material is needed ~~to be~~ for a better fit to the observed field.

Scenario 3 ~~has been~~was judged ~~the best to represent~~ as the basin ~~geological~~ structure ~~of the basin that~~ that best reproduces the gravity signature of the Yerrida Basin. Of course, ~~S~~some issues remain with the model as shown in Figure 12~~Figure 14~~ and presented in the Discussion.

5 Discussion

The process of collating, interpreting and modelling geoscientific data leads to a greater understanding of the capabilities of the available data. ~~This expands the existing knowledge of the target region which can then inform decisions for future data collection, interpretation and modelling. The~~ The greatest amount of knowledge typically gained by the geoscientist performing these exercises, however ~~gains all this knowledge, but~~ whether this knowledge can then be effectively communicated so others benefit is challenging (Quigley et al., 2019). The discussion that follows attempts to do this by first presenting a range of outcomes that were considered useful. Some of these outcomes are not 'successful' in the traditional sense, but nonetheless are worthwhile reporting, in particular which datasets were useful for different purposes, where limitations exist, and what aspects of the range of modelling procedures nonetheless provided useful insight. The second part of the discussion is a synthesis of what was learned about the structure of the Yerrida Basin and potential for mineralisation.

5.1 Alternatives for Higher Density Material

~~The structural and lithological interpretation, augmented by existing GSWA mapping (WAROX) and field validation provided input to the 3D model.~~ The central aim was to determine if the characteristic density signature of the Yerrida Basin was due to ~~more~~ extensive mafic rocks at depth or some other geological reason, such as diagenetic or near-surface alteration. Such non-magmatic processes that are plausible in the Yerrida Basin region is the presence of dolomite. Dolomitsation of carbonate rocks forms dolostone when calcite ions are replaced by magnesium ions. Calcite (mean density = 2.71 gm/cm^3) is less dense than dolomite (mean density = 2.84 gm/cm^3), thus dolomitisation is expected to increase the density of a rock. The magnitude of density increase depends on the carbonate proportion of the original rock (with lower proportions resulting in less carbonate to dolomitise, and thus a smaller density increase) combined with the degree that dolomitisation has occurred. ~~An alternative already briefly introduced considered that later diagenetic or near-surface alteration caused this increase in density. Dolomitsation of carbonate rocks forms dolostone when calcite ions are replaced by magnesium ions. Calcite (mean density = 2.71 gm/cm^3) is less dense than dolomite (mean density = 2.84 gm/cm^3), thus dolomitisation is expected to increase the density of a rock. The magnitude of density increase depends on the carbonate proportion of the original rock (with lower proportions resulting in less carbonate to dolomitise, and thus a smaller density increase) combined with the degree that dolomitisation has occurred.~~

3D geophysical inversion was employed to explore both these scenarios, and the recovered density distribution leads us to which is more plausible. Region 1 required a significant increase in density when compared to the prior geological model to account for the density anomalies seen in the observed gravity data (Figure 11~~Figure 13~~b-d – ~~middle~~ centre panels). The Juderina Formation forms a significant unit in this area, both in outcrop and at depth and is likely to contain dolomitic rocks. The carbonate portion of the Juderina Formation includes the relatively minor Bubble Well member and is not considered large enough (Occhipinti et al., 2017) to account for the gravity anomaly. In addition, the magnitude of densities required to produce the required anomaly (>2.9 ~~gms~~g/cm^3) is higher than is realistic for dolostone, even if the rock was made entirely of dolomite. Thus, an extensive mafic component in the subsurface is a more likely source of the gravity anomaly in this location (Figure 12a). Modelling in ~~r~~Region 2 (Figure 11~~Figure 13~~b-d – ~~middle~~ centre panels; ~~Figure 13~~Figure 12b~~a, b~~) also supports this reasoning, with an additional ~~large~~ large high~~-~~ density (>2.9 ~~gms~~g/cm^3) body required to account for the observed gravity data. Here, the Juderina Formation is not as extensive as in ~~r~~Region 1, and the position of the recovered density anomaly implies a closer spatial association with the Killara Formation at depth (Figure 11d).~~.~~

5.2 Density Distribution and Geological Implications

The distribution of mafic units in the Yerrida Basin was determined through geological modelling combined with petrophysically constrained gravity inversion. The distribution of these mafic units ~~determined from modelling~~ is shown in Figure 13~~Figure 15~~, along with the previously assumed extents of mapped and interpreted Killara Formation for comparison. The Juderina Formation likely hosts the additional mafic units. We acknowledge that other formations may also host mafic rocks; just the observations to support this hypothesis have not been made. Figure 13 also ~~Also shown are~~ displays r~~r~~egions 1 and 2 from Figure 11~~Figure 13~~, and two new regions, ~~r~~Region 3, defined by the area of misfit (Figure 12~~Figure 14~~b) and R~~r~~egion 4, which will be discussed later in this section. The grey regions indicate our current knowledge of the extent of the Killara Formation as shown on GSWA maps and geophysical interpretation and can be assumed to only represent outcrop or near-surface (<50m below depth below surface) rocks. The coloured cells are outputs from the final inversion voxet, and represent the predicted extents of mafic material at the surface and at depth. Cell colour indicates different high-density bodies ~~-~~added incrementally to the prior geological model in scenarios 2 and 3, but have no other significance. The plan view shows a significant increase in the extent of mafic material from our current understanding. Region 4 is an extensive northeast-trending body of mafic material modelled as Killara Formation.

~~A series of 3D isometric views both above and below the geological model as determined by inversion are shown in~~ Figure 14~~Figure 16~~a displays the inverted model of the Yerrida Basin viewed from the southwest, with only basin rocks and Archean greenstones displayed for ease of visualiation. ~~These views are all from the southwest and show the depth extent of inverted geological units.~~ Of note is the depth extent of both the Juderina Formation and mafic material ~~are the mafic units a~~in Region 4.~~s depicted in the right-hand panels. The panels on the right show the distribution of mafic material, with the o~~ The section view (Figure 14~~Figure 14~~b) shows on the basin rocks and proposed mafic material. ~~ther units (sedimentary, granite-gneiss and greenstones) filtered out to allow better visualisation.~~ The mafic units are ~~bodies were modelled~~

individually and coloured-coded to differentiate those that were progressively added incrementally during scenario testing. The different colours are not intended to indicate that any particular unit is unique in stratigraphic position or composition.

Most of the higher density, mafic material is located close to the surface (Figure 14Figure 14b);. howeverhowever, some . The mafic material in region 4 is shown has been determined to extend deeper in the southwest part (Figure 14Figure 16bd).

This interpretation is consistent with the gravity modelling and interpretation of Hackney (2004), who suggests the Yerrida Basin deepens and extends under the Byrah-Padbury Basin to the north. Here the higher density material could be part of the Killara Formation, or a substantial part of the mafic component to the Juderina Formation. Figure 14Figure 16b also 'A' also shows the Juderina Formation to be is very thick (>10km, and up to 20 20km, off-section) with deeper parts to the and deepens towards the northeast. 20 Twenty km kkilometres is almost certainly too thickimplausible given the thickness estimates of Pirajno and Adamides (2000). The incorrect mis-estimateand is likely due to a combination of artefacts resulting from inversion and the presence of thick (~7km) and dense Narracoota Formation rocks (Pirajno et al., 1998) hosted in the hanging wall of the Goodin Fault to the northwest interfering with the reconciliation of the calculated gravity response to the observed gravity response. Nonetheless, it indicates that a thicker portion of the Yerrida Basin probably exists here, just that the thickness is difficult to determine geophysically without guidance in the form of detailed sedimentological analysis.

5.3 Distinguishing Mafic Rocks Using Chemical Composition

Geophysical inversion has been useful in revising the extent of mafic rocks in the Yerrida Basin. What geophysics cannot do with our current dataset is determine whether the interpreted mafic rocks all belong to the Killara Formation, or whether the mafic rocks have different compositions and thus reveal a more complex stratigraphy. The major and trace chemical composition of whole rock samples has been obtained from drillcore (THD001, DGDD347 and the GSWA Geochemistry Database "WACHEM"), surface samples (UWA field work and WACHEM) with analysis and compilation by Olierook et al. (2018) to help us achieve this aim.

As DGDD347 is close to the northern boundary of the Yerrida Basin (Figure 1Figure 1), and samples both Bryah and Yerrida Basin rocks. Thus, wwe were able to check use these samples to establish whether any of the mafic rocks sampled in the Juderina Formation are sills or dykes related to the Narracoota Formation. Figure 17Figure 15a shows the geochemical distribution of mafic rocks sampled from the Yerrida and Byrah-Padbury basins on a basaltic Th/Yb vs Nb/Yb diagram (Pearce, 2014). This type of diagram is usually used to recognise sources of magma to provide insight into the tectonic setting that generated them, with higher Th/Yb representing lavas modified by subduction-related processes, and those with higher Nb/Yb showing increasing levels of crustal contamination. While possible, interpreting such settings from these results is speculative and as more detailed stratigraphic and volcanological work would be required for a definitive answersupport. Nonetheless, the diagram proves useful in discriminating between different types of mafic rocks in the region that may have formed at different times and/or in different tectonic settings.

Samples from drillhole DDGD347DGDD347 ("DG") and THD001 ("THD") are clustered toward the higher end of both ratios. Most of the DG and THD samples are close to, but not within, the mid-ocean ridge basalt-ocean-island basalt

Formatted: Caption, Line spacing: 1.5 lines

(MORB-OIB) array. Importantly, the DG and THD samples are distinctive in their tight clustering and position with respect to the Narracoota and Killara formation samples (Olierook et al., 2018), meaning they are different geochemically, and were thus likely generated in a different setting. This interpretation is supported by Figure 15b ~~Figure 17b, a similar diagram to Figure 17a, but uses a~~ which displays the TiO_2/Yb ratio on the y-axis as a proxy for deep melting (Pearce, 2008). Here, the DG and THD samples are distinguishable from the Killara and Narracoota formations based on both the TiO_2/Yb and Nb/Yb ratios. DG and THD can also be separated into their own classifications. The DG samples fall within the alkali classification, while the THD samples are mostly classified as tholeiitic basalts. The DG and THD samples have a deep melting signature, whereas most of the Killara and Narracoota samples have a shallow melting signature.

The overall non-arc melting signature of ~~Figure 17~~Figure 15b is similar to the interpretation of Olierook et al. (2018) that mafic magmatism in the southern Capricorn region was interpreted to be generated in an intracontinental rift setting. Our results show that the while the larger tectonic setting may not have changed, the magmatic history of the southern Capricorn is likely more protracted, complex and punctuated by periods of mafic magmatism with a changing source (Occhipinti et al., 2017;Occhipinti et al., 1997;Pirajno and Occhipinti, 2000).

5.4 Yerrida Basin Mineralisation

Geochemistry can provide insight to the prospectivity of mafic rocks for VMS mineralisation. Flat REE profiles are typical for VMS prospectivity (Hawke, 2016;Hawke et al., 2015) however, both spider diagrams for THD (Figure 16a) **and DG** (Figure 16b) **show inclined, and thus VMS-un-prospective REE profiles** ~~(~~ ~~Figure 18)~~**.** These observations are also made by Mueller (2011) for drill hole THD001. An example of a flat REE pattern from basaltic and micro-gabbroic rocks sampled from the Degrussa mine are shown in grey for reference (Hawke, 2016).

5.5 Basin Development

The location of the thicker mafic and sedimentary portion of the basin is juxtaposed against the Goodin Fault. The thicker part of the Yerrida Basin may then represent a deepening of the basin toward the northwest, which occurred during c. 2200 – c. 2000 Ma lithospheric extension and rifting (Occhipinti et al., 2017;Pirajno and Adamides, 2000;Pirajno and Occhipinti, 2000). The mafic component of rifting may have manifested in two forms. Extensive magmatism contemporaneous with the deposition of: (1) the Juderina Formation or (2) the Killara Formation during development of the Mooloogool Group.

A period of extensive mafic volcanism at c. 2045 Ma saw mafic rocks of the Narracoota Formation intrude and overly the Karalundi Formation in the Bryah Sub-basin located to the north and northwest of our study area (Hawke et al., 2015). Occhipinti et al. (2017) suggest that the Killara and Narracoota formations are manifestations of magmatism during rifting in different basin depocentres that temporally overlap. This is supported by Pirajno and Adamides (2000) who interpret the Killara Formation as basalts extruded in a continental setting, with geochemical affinities similar to the hyloclastites of the Narracoota Formation. Gravity modelling performed and interpreted by Pirajno and Occhpinti (1995) and Pirajno and

Formatted: Font: 10 pt, Not Bold
Formatted: Font: 10 pt, Not Bold
Formatted: Font: 10 pt, Not Bold
Formatted: Font: 10 pt, Not Bold
Formatted: Font: 10 pt, Not Bold, Not Superscript/ Subscript
Formatted: Font: 10 pt, Not Bold
Formatted: Font: 10 pt, Not Bold, Not Superscript/ Subscript
Formatted: Font: 10 pt, Not Bold
Formatted: Font: 10 pt, Not Bold
Formatted: Font: 10 pt, Not Bold
Formatted: Font: 10 pt
Formatted: Line spacing: 1.5 lines
Formatted: Font: 10 pt
Formatted: Font: 10 pt
Formatted: Default Paragraph Font, Font: 10 pt
Formatted: Font: Not Bold
Formatted: Default Paragraph Font, Font: 10 pt
Formatted: Font: Not Bold
Formatted: Default Paragraph Font, Font: 10 pt
Formatted: Default Paragraph Font, Font: 10 pt
Formatted: Default Paragraph Font, Font: 10 pt, Not Bold
Formatted: Default Paragraph Font, Font: Not Bold
Formatted: Default Paragraph Font

Occhipinti (1998) who find the Narracoota Formation thickens up to seven km northwest ~~toward the south of the~~ of the Goodin Fault. If the high density material modelled here is part of the Killara Formation, then thickening of the mafic Narracoota Formation toward the south, and thickening of the Killara Formation toward the northwest supports the suggestion of Occhipinti et al. (2017) that the current position of Goodin Fault may represent a rift axis and volcanic vent for this period of magmatism.

Regions 1, 2 and 3 identified from the modelled high-density material are thick may ~~and suggest additional sites that may~~ represent vents sites of accumulation of mafic material~~and the source of mafic volcanism~~ (Figure 11~~Figure 13~~b and d). Region 1 is primarily hosted within Juderina Formation and the high-density region recovered from inversion may represent the mafic component of that formation. Regions 2 and 3 have been modelled to be ~~are~~ hosted within the Mooloogool Group rocks due to the prevalence of these formations these areas, and thus ~~may be more~~ more plausibly to be ~~likely to be~~ associated with the ~~composed of~~ Killara Formation. Regions 1 and 2 may represent vent sites ~~The thickness of the basin around Regions 2 and 3 is modelled to be thicker than elsewhere, and may represent another rift, smaller than the one encedirect.com/science/article/B6V6S-4SWFNTJ-1/2/af2ae6e605655e8157d6516c7536aa41</url></related-urls></urls></record></Cite></EndNote>(Calcagno et al., 2008)[illegible]. The purpose paleotopographic low, in which sedimentary and mafic material with provenance from elsewhere was deposited.~~ for mafic magmatism due to the proposed relative abundance of mafic material however this hypothesis, as will be shown, is less plausible when considered with sulphur isotopic data.

Multiple sulphur isotopic analysis (LaFlamme et al., In review;LaFlamme et al., 2018) show that the non-Killara Yerrida Basin mafic volcanic rocks have a slight negative Δ33S signature, typical of Paleoproterozoic basins (Johnston et al., 2006). It suggests that these magmas have not interacted with the Archean basement during volcanism. Given the proximity of Archean basement to these rocks, this is somewhat enigmatic and further suggests that magmas were sourced from the deeper parts of the basin. This source region is likely to the north and northwest of the Yerrida Basin where Archean basement (i.e. Yilgarn Craton) is likely absent, or along the Goodin Fault (Figure 17~~Figure 19~~). Yerrida Basin magmatism was likely contemporaneous with that related to Narracoota Formation (Pirajno and Occhipinti, 2000) albeit via different vents (Occhipinti et al., 2017).

Figure 17~~Figure 19~~b shows the proposed locations of vents for non-Killara magmatism, broadly estimated based on the gravity anomaly and away from Archean rocks. Higher ~~amplitude~~magnitude gravity anomalies are typically associated with locations proximal to vents due to the greater amounts of high-density material, while the vents themselves exhibit a lower magnitude anomaly due to the lack of high-density material around the crater (Blaikie et al., 2014;Blaikie et al., 2012). The gravity signature is unlikely to reveal short wavelengths that would indicate this geometry at the scale of this study, due to both data resolution and burial of these vents under the Padbury Basin, thus vent location is likely to be in areas of higher overall gravity anomaly. These vents are also a plausible source for the mafic intrusive and extrusive Killara Formation, however isotopic data is required to support this interpretation. Pirajno and Occhipinti (2000) and Occhipinti et al. (2017) provide an some explanation to the volcanology of the Killara Formation.

Transport of magmas would likely have occurred along major structures (e.g. the Goodin Fault) or as sills along rock unit contacts. These near-surface magmatic pathways would have transported material around the Archean Goodin and Marymia inliers. Given the supposition that sill intrusion is restricted to the Juderina Formation, it is suggested that the Juderina Formation also extends to the northwest beyond the current extents of the Yerrida Basin (Figure 17~~Figure 19, a and b~~Figure 18). This reasoning supports the interpretation of Occhipinti et al. (2017) that the Yerrida Basin underlies the current day location of the Bryah sub-basin and Padbury Basin.

The position of vents near the Goodin Fault or in the current-day Bryah sub-basin presents an interesting question to how magmatic rocks traversed the potential barrier the Goodin Fault may have represented and were deposited in the current-day Yerrida Basin region. We propose that development of the Goodin Fault played an important role in the early architecture of the Yerrida Basin. Figure 18a shows how magmatism and deposition of Windplain and Mooloogool rocks occurred either side of the present-day location of the Goodin Fault under regional extension. The Goodin Fault is considered to have formed from a rift that was generated from early tectonic extension (Occhipinti et al., 2017). This proto-Goodin Fault would not have produced significant paleotopography, and lava flows and intrusions generated from the proposed vent locations were then able extend to the current Yerrida Basin extents shown in southeast of Figure 18a. Continued extension and normal-faulting formed the Goodin Fault in roughly its present day location (Figure 18b). Partitioning of the early Yerrida Basin occurred, and deposition of Byrah sub-basin rocks is located northwest of the Goodin Fault. Magmatism continued through vents in the northwest (Figure 18c) but any lava flows would have been restricted to regions northwest of the Goodin Fault.

5.6 Application to Other Regions

The approach described in this paper ~~can be applied~~is applicable to other rift-basin regions located on the margins of cratons that host cryptic geophysical anomalies. The Volta Basin is such an example, where rifts have been interpreted from gravity and magnetic data and density anomalies suggest in-fill from mafic volcanic rocks (Reichelt, 1971;Álvaro and Vizcaïno, 2012), however their three-dimensional distribution and plausibility of the interpretation is not well understood (Jessell et al., 2016). Likewise, the structure of South American cratonic basins remains cryptic (Braitenberg et al., 2007), though recent studies modelling gravity data have shown progress in gaining geological understanding in these regions (Sanchez-Rojas and Palma, 2014).

6 Conclusions

This ~~A~~ comprehensive ~~structural and geophysical~~ study of the Yerrida Basin, southern Capricorn Orogen demonstrates how mapping undercover can be conducted. ~~was completed~~A set of geophysical and 3D modelling techniques demonstrate hypothesis development and testing.~~.~~ We show how the integration of ~~A variety of g~~geophysical, geological and geochemical datasets ~~has been~~ can ~~used to~~ achieve a better understanding of basin architecture and magmatic history.

~~Structural interpretation with magnetic data was hindered by low- to no-contrast susceptibility and flat-lying geology; however, the AEM data provided by the Capricorn TEMPEST Geophysical Survey gave critical support to lithological interpretation.~~

A widespread gravity anomaly spatially associated with sedimentary basin rocks was investigated to infer that a considerable high-density component was required that was incompatible with known exposure of high-density rocks and stratigraphic understanding. The hypothesis that the higher density anomaly may be linked to mafic rock bodies was investigated using a set of forward modelling and inversion techniques. First, a conceptual 3D model around the Goodin Inlier was constructed in a kinematic modelling package to evaluate whether a higher density component was required to recreate the observed gravity response. 3D forward modelling showed that a layer of mafic material up a 2000 m thick is required to produce a similar response to the observed response. These results were encouraging but deemed too simple to adequately test the likely more complex architecture the gravity data represented.

2D section forward modelling was then used to investigate a transect across the Goodin Inlier to test whether intrusions associated with the Killara Formation (such as dykes and sills) were plausible candidates to produce the necessary gravity response. This was confirmed as plausible, so a basin-scale 3D model was constructed as a prior model for inversion to test where other high-density bodies were throughout the rest of the basin. Gravity inversions were conducted in a systematic procedure that progressively added mafic bodies to ~~systematically~~ understand the sensitivity of misfit to the observed gravity and increased volume of higher density bodies. Thus, our results show that the mafic composition of the Yerrida Basin is likely to be significantly larger than is shown on current maps and represented by the published stratigraphy.

Geochemistry was used to analyse whether mafic units logged in the Juderina Formation from drillcore were the intrusive part of the Killara Formation, which they are not. Geochemistry also showed that these rocks are not prospective for VHMS-style mineralisation. A localised different set of mafic bodies was revealed suggesting substantial mafic activity associated with the Juderina Formation that does not contain an Archean signature. The proximity of Archean basement suggests that the sources of magmatism ~~was not in the~~at the northern edges of basin, ~~itself, but at the northern edge~~ either under the Bryah sub-basin and Padbury Basin, or along large structures such as the Goodin Fault.

7 Appendices

Table A 1. Geological data that aided construction of the forward model shown in Figure 9~~Figure 11~~. SOP = Start-of-profile.

Distance SOP m	Structure	Name	Rock W	Rock E
0	***SOP***			
550	Fault	Jenkin Fault	Narracoota	Karalundi
1600	Fault	Murchison Fault	Karalundi	Karalundi
6600	Fault	Goodin Fault	Karalundi	Doolgunna
8150	Contact		Doolgunna	Mt Leake
10350	Contact		Mt Leake	Doolgunna

11100	Contact		Doolgunna	Johnson Cairn
11750	Fault		Johnson Cairn	Johnson Cairn
13150	Fault		Johnson Cairn	Johnson Cairn
13250	Contact		Johnson Cairn	Juderina
13550	Contact		Juderina	Johnson Cairn
14150	Fault		Johnson Cairn	Johnson Cairn
18600	Fault		Johnson Cairn	Johnson Cairn
21900	Contact		Johnson Cairn	Juderina
23000	Contact		Juderina	Goodin Inlier
25000	Fault		Goodin Inlier	Goodin Inlier
25500	Fault		Goodin Inlier	Goodin Inlier
26150	Fault		Goodin Inlier	Goodin Inlier
32000	Fault		Goodin Inlier	Goodin Inlier
32250	Fault		Goodin Inlier	Goodin Inlier
33750	Fault		Goodin Inlier	Goodin Inlier
40550	Contact		Goodin Inlier	Juderina (mag)
41800	Contact		Juderina (mag)	Johnson Cairn
45500	Fault		Johnson Cairn	Johnson Cairn
45800	Contact		Johnson Cairn	Doolgunna
50000	Fault		Doolgunna	Doolgunna
53300	Contact		Doolgunna	Killara
53800	Contact		Killara	Doolgunna
55000	***EOP***			

8 Data Availability

8.1 3D models

The Yerrida Basin model is supplied in Geomodeller format and available from DOI: 10.5281/zenodo.3245772.

8.2 Noddy

Noddy software, models and their gravity forward response are provided in native format from DOI: 10.5281/zenodo.3245788. A download for Windows installation of Noddy is available from http://tectonique.net/noddy/.

9 Author Contribution

ML performed the data compilation, modelling, analyses, interpretation and manuscript preparation. SO contributed to analyses, geological background and interpretations. CL contributed to geochemical data compilation, analyses and

interpretation. AA assisted with geophysical data compilation, preparation and interpretation. LR performed the petrophysical analyses and data ~~compliation~~compilation. All authors contributed to manuscript drafting.

10 Competing Interests

The authors declare that they have no conflict of interest.

11 Acknowledgements

MDL thanks the Geological Survey of Western Australia, the Minerals Research Institute of Western Australia and the Australian Research Council (DE190100431) for their support. Thank you to Paul Hilliard (Sandfire Resources) for his invitation to the DeGrussa mine, valuable discussion and supply of geochemical data. Thank you to Camilla Sørensen and Tim Munday (CSIRO) for their assistance with ~~AEM data and imaging (AEM section Figure 8a).~~geophysical interpretation and analysis. Petrophysical analysis was performed in the UWA petrophysics lab with thanks to Cam Adams. Funding for this work was from a West Australian Government Exploration Incentive Scheme grant awarded to UWA from the Geological Survey of Western Australia and the 'Distal Footprints of Giant Ore Systems - UNCOVER Australia', CSIRO Science & Industry Endowment Fund (SIEF).

12 References

Aitken, A. R. A., and Betts, P. G.: High-resolution aeromagnetic data over central Australia assist Grenville-era (1300 Ma-1100 Ma) Rodinia reconstructions, Geophys. Res. Lett., 35, 2008.

Aitken, A. R. A., and Betts, P. G.: Multi-scale integrated structural and aeromagnetic analysis to guide tectonic models: An example from the eastern Musgrave Province, Central Australia, Tectonophysics, 476, 418-435, 2009.

Almalki, K. A., Ailleres, L., Betts, P. G., and Bantan, R. A.: Evidence for and relationship between recent distributed extension and halokinesis in the Farasan Islands, southern Red Sea, Saudi Arabia, Arabian Journal of Geosciences, 8, 8753-8766, 10.1007/s12517-015-1792-9, 2015.

Álvaro, J. J., and Vizcaïno, D.: Proterozoic microbial reef complexes and associated hydrothermal mineralizations in the Banfora Cliffs, Burkina Faso, Sedimentary Geology, 263-264, 144-156, 2012.

Bagas, L.: Early tectonic history of the Marymia Inlier and correlation with the Archaean Yilgarn Craton, Western Australia, Australian Journal of Earth Sciences, 46, 115-125, 10.1046/j.1440-0952.1999.00691.x, 1999.

Betts, P., Williams, H., Stewart, J., and Ailleres, L.: Kinematic analysis of aeromagnetic data: Looking at geophysical data in a structural context, Gondwana Research, 11, 582-583, 2007.

Betts, P. G., Valenta, R. K., and Finlay, J.: Evolution of the Mount Woods Inlier, northern Gawler Craton, Southern Australia: an integrated structural and aeromagnetic analysis, Tectonophysics, 366, 83-111, 2003.

Blaikie, T. N., Ailleres, L., Cas, R. A. F., and Betts, P. G.: Three-dimensional potential field modelling of a multi-vent maar-diatreme — The Lake Coragulac maar, Newer Volcanics Province, south-eastern Australia, Journal of Volcanology and Geothermal Research, 235-236, 70-83, https://doi.org/10.1016/j.jvolgeores.2012.05.002, 2012.

Formatted: Space After: 6 pt

Blaikie, T. N., Ailleres, L., Betts, P. G., and Cas, R. A. F.: A geophysical comparison of the diatremes of simple and complex maar volcanoes, Newer Volcanics Province, south-eastern Australia, Journal of Volcanology and Geothermal Research, 276, 64-81, https://doi.org/10.1016/j.jvolgeores.2014.03.001, 2014.

Blewett, R. S., Czarnota, K., and Henson, P. A.: Structural-event framework for the eastern Yilgarn Craton, Western Australia, and its implications for orogenic gold, Precambrian Research, 183, 203-229, 10.1016/j.precamres.2010.04.004, 2010.

Braitenberg, C., Wienecke, S., Ebbing, J., Born, W., and Redfield, T.: Joint Gravity and Isostatic Analysis for Basement Studies–A Novel Tool, 2007, 15-18,

Brethes, A., Guarnieri, P., Rasmussen, T. M., and Bauer, T. E.: Interpretation of aeromagnetic data in the Jameson Land Basin, central East Greenland: Structures and related mineralized systems, Tectonophysics, 724-725, 116-136, https://doi.org/10.1016/j.tecto.2018.01.008, 2018.

Briggs, I. C.: Machine contouring using minimum curvature, Geophysics, 39, 39-48, 1974.

Calcagno, P., Chilès, J. P., Courrioux, G., and Guillen, A.: Geological modelling from field data and geological knowledge: Part I. Modelling method coupling 3D potential-field interpolation and geological rules, Physics of the Earth and Planetary Interiors, 171, 147-157, 2008.

Clark, D. A.: Magnetic petrophysics and magnetic petrology: aids to geological interpretation of magnetic surveys, ASGO Journal of Australian Geology and Geophysics, 17, 83–103, 1997.

Cudahy, T. J., Jones, M., Thomas, M., Laukamp, C., Caccetta, M., Hewson, R., Rogdger, A., and Verrall, M.: Next generation mineral mapping: Queensland Airborne Hymap and Satellite ASTER Surveys 2006-2008. CSIRO report P2007/364, 153, 2008.

de Kemp, E., Jessell, M., Ailleres, L., Schetselaar, E., Hillier, M., Lindsay, M. D., and Brodaric, B.: Earth model construction in challenging geologic terrain: Designing workflows and algorithms that makes sense, Exploration 17: Sixth Decennial International Conference on Mineral Exploration, Toronto, 2017.

Dufréchou, G., Harris, L. B., and Corriveau, L.: Tectonic reactivation of transverse basement structures in the Grenville orogen of SW Quebec, Canada: Insights from gravity and aeromagnetic data, Precambrian Research, 241, 61-84, https://doi.org/10.1016/j.precamres.2013.11.014, 2014.

Fairhead, J. D.: The structure of the lithosphere beneath the Eastern rift, East Africa, deduced from gravity studies, Tectonophysics, 30, 269-298, http://dx.doi.org/10.1016/0040-1951(76)90190-6, 1976.

Fullagar, P. K., Pears, G., Hutton, D., and Thompson, A.: 3D gravity and aeromagnetic inversion for MVT lead-zinc exploration at Pillara, Western Australia, Exploration Geophysics, 35, 142-146, doi:10.1071/EG04142, 2004.

Giraud, J., Lindsay, M., Ogarko, V., Jessell, M., Martin, R., and Pakyuz-Charrier, E.: Integration of geoscientific uncertainty into geophysical inversion by means of local gradient regularization, Solid Earth, 10, 193-210, 10.5194/se-10-193-2019, 2019.

Giraud, J., Lindsay, M., Jessell, M., and Ogarko, V.: Towards plausible lithological classification from geophysical inversion: Honouring geological principles in subsurface imaging, Solid Earth, 11, 419-436, 10.5194/se-11-419-2020, 2020.

Grant, F. S.: Aeromagnetics, geology and ore environments, I. Magnetite in igneous, sedimentary and metamorphic rocks: An overview, Geoexploration, 23, 303-333, 10.1016/0016-7142(85)90001-8, 1985.

Guillen, A., Calcagno, P., Courrioux, G., Joly, A., and Ledru, P.: Geological modelling from field data and geological knowledge: Part II. Modelling validation using gravity and magnetic data inversion, Physics of the Earth and Planetary Interiors, 171, 158-169, 2008.

Gunn, P. J.: Quantitative methods for interpreting aeromagnetic data: a subjective review, AGSO Journal of Australian Geology and Geophysics, 17, 105-114, 1997.

Hackney, R.: Gravity anomalies, crustal structure and isostasy associated with the Proterozoic Capricorn Orogen, Western Australia, Precambrian Research, 128, 219-236, http://dx.doi.org/10.1016/j.precamres.2003.09.012, 2004.

Hawke, M. L., Meffre, S., Stein, H., Hilliard, P., Large, R., and Gemmell, J. B.: Geochronology of the DeGrussa volcanic-hosted massive sulphide deposit and associated mineralisation of the Yerrida, Bryah and Padbury Basins, Western Australia, Precambrian Research, 267, 250-284, http://dx.doi.org/10.1016/j.precamres.2015.06.011, 2015.

Hawke, M. L.: The Geological Evolution of the DeGrussa volcanic-hosted massive sulfide deposit and the Eastern Capricorn Orogen, Western Australia, PhD, Centre for Ore Deposit and Earth Sciences, School of Physical Sciences, The University of Tasmania, Hobart, Tasmania, 434 pp., 2016.

Hildenbrand, T. G., Berger, B., Jachens, R. C., and Ludington, S.: Regional Crustal Structures and Their Relationship to the Distribution of Ore Deposits in the Western United States, Based on Magnetic and Gravity Data, Economic Geology, 95, 1583-1603, 10.2113/95.8.1583, 2000.

Husson, E., Guillen, A., Séranne, M., Courrioux, G., and Couëffé, R.: 3D Geological modelling and gravity inversion of a structurally complex carbonate area: application for karstified massif localization, Basin Research, 30, 766-782, 10.1111/bre.12279, 2018.

Jessell, M.: Noddy - an interactive map creation package, MSc, University of London, 52 pp., 1981.

Jessell, M., Aillères, L., de Kemp, E., Lindsay, M., Wellmann, F., Hillier, M., Laurent, G., Carmichael, T., and Martin, R.: Next Generation Three-Dimensional Geologic Modeling and Inversion, Society of Economic Geologists: Special Publication 18, 261-272, 2014.

Jessell, M. W., and Valenta, R. K.: Structural geophysics: Integrated structural and geophysical modelling, in: Computer Methods in the Geosciences, edited by: Declan, G. D. P., Pergamon, 303-324, 1996.

Jessell, M. W., Begg, G. C., and Miller, M. S.: The geophysical signatures of the West African Craton, Precambrian Research, 274, 3-24, https://doi.org/10.1016/j.precamres.2015.08.010, 2016.

Johnston, D. T., Poulton, S. W., Fralick, P. W., Wing, B., Canfield, D. E., and Farquhar, J.: Evolution of the oceanic sulfur cycle at the end of the Paleoproterozoic, Geochimica et Cosmochimica Acta, 70, 5723-5739, 2006.

Kohanpour, F., Lindsay, M. D., Occhipinti, S., and Gorczyk, W.: Structural controls on proterozoic nickel and gold mineral systems identified from geodynamic modelling and geophysical interpretation, east Kimberley, Western Australia, Ore Geology Reviews, 95, 552-568, https://doi.org/10.1016/j.oregeorev.2018.03.010, 2018.

Kovesi, P.: Phase Preserving Tone Mapping of Non-Photographic High Dynamic Range Images, 2012 International Conference on Digital Image Computing Techniques and Applications (DICTA), 2012, 1-8,

LaFlamme, C., Fiorentini, M. L., Lindsay, M. D., and Bui, T. H.: Atmospheric sulfur is recycled to the crystalline continental crust during supercontinent formation, Nature Communications, 9, 4380, 10.1038/s41467-018-06691-3, 2018.

LaFlamme, C., Fiorentini, M., and Beaudoin, B. C.: Insight into the seawater sulfate reservoir at 2.0 Ga from the Paleoproterozoic Degrussa Cu-Au volcanogenic massive sulfide deposit, Geochimica et Cosmochimica Acta, In review.

Lindsay, M. D., Aillères, L., Jessell, M. W., de Kemp, E. A., and Betts, P. G.: Locating and quantifying geological uncertainty in three-dimensional models: Analysis of the Gippsland Basin, southeastern Australia, Tectonophysics, 546–547, 10-27, 10.1016/j.tecto.2012.04.007, 2012.

Lindsay, M. D., Occhipinti, S., Aitken, A. R. A., Metelka, V., Hollis, J., and Tyler, I.: Proterozoic accretionary tectonics in the east Kimberley region, Australia, Precambrian Research, 278, 265-282, http://dx.doi.org/10.1016/j.precamres.2016.03.019, 2016.

Lindsay, M. D., Spratt, J., Occhipinti, S. A., Aitken, A. R. A., Dentith, M. C., Hollis, J. A., and Tyler, I. M.: Identifying mineral prospectivity using 3D magnetotelluric, potential field and geological data in the east Kimberley, Australia, Geological Society, London, Special Publications, 453, 10.1144/sp453.8, 2017.

Manger, G. E.: Porosity and bulk density of sedimentary rocks: Contributions to geochemistry, Geological Survey Bulletin, 1144-E, E1-E55, 1963.

Mueller, D. H. A.: Final report on drilling of THD001: a 1017.8 m vertical core hole on E52/1673: GSWA reference C144/2005, Sipa Exploration NL, 2011.

Nettleton, L. L.: Gravity and magnetic calculations, Geophysics, 7, 293-310, 1942.

Occhipinti, S., Hocking, R., Lindsay, M., Aitken, A., Copp, I., Jones, J., Sheppard, S., Pirajno, F., and Metelka, V.: Paleoproterozoic basin development on the northern Yilgarn Craton, Western Australia, Precambrian Research, 300, 121-140, http://dx.doi.org/10.1016/j.precamres.2017.08.003, 2017.

Occhipinti, S. A., Grey, K., Pirajno, F., Adamides, N. G., Bagas, L., Dawes, P., and Le Blanc-Smith, G.: Stratigraphic revision of the Palaeoproterozoic rocks of the Yerrida, Bryah and Padbury Basins (formerly Glengarry Basin), 1997.

Olierook, H. K. H., Sheppard, S., Johnson, S. P., Occhipinti, S. A., Reddy, S. M., Clark, C., Fletcher, I. R., Rasmussen, B., Zi, J.-W., Pirajno, F., LaFlamme, C., Do, T., Ware, B., Blandthorn, E., Lindsay, M., Lu, Y.-J., Crossley, R. J., and Erickson, T. M.: Extensional episodes in the Paleoproterozoic Capricorn Orogen, Western Australia, revealed by petrogenesis and geochronology of mafic–ultramafic rocks, Precambrian Research, 306, 22-40, https://doi.org/10.1016/j.precamres.2017.12.015, 2018.

Pearce, J. A.: Geochemical fingerprinting of oceanic basalts with applications to ophiolite classification and the search for Archean oceanic crust, Lithos, 100, 14-48, https://doi.org/10.1016/j.lithos.2007.06.016, 2008.

Pearce, J. A.: Immobile Element Fingerprinting of Ophiolites, Elements, 10, 101-108, 10.2113/gselements.10.2.101, 2014.

Perrouty, S., Aillères, L., Jessell, M. W., Baratoux, L., Bourassa, Y., and Crawford, B.: Revised Eburnean geodynamic evolution of the gold-rich southern Ashanti Belt, Ghana, with new field and geophysical evidence of pre-Tarkwaian deformations, Precambrian Research, 204-205, 12-39, 2012.

Pirajno, F., and Occhpinti, S. A.: Bryah, W.A. Sheet 2646: 1:100 000 Geological Series, Western Australia Geological Survey, 1995.

Pirajno, F., and Occhipinti, S. A.: Geology of the Bryah 1:100 00 sheet., Geological Survey of Western Australia, 1998.

Pirajno, F., Occhipinti, S. A., and Swager, C. P.: Geology and tectonic evolution of the Palaeoproterozoic Bryah, Padbury and Yerrida basins (formerly Glengarry Basin), Western Australia: implications for the history of the south-central Capricorn Orogen, Precambrian Research, 90, 119-140, 10.1016/S0301-9268(98)00045-X, 1998.

Pirajno, F., and Occhipinti, S. A.: Three Palaeoproterozoic basins-Yerrida, Bryah and Padbury-Capricorn Orogen, Western Australia, Australian Journal of Earth Sciences, 47, 675-688, 10.1046/j.1440-0952.2000.00800.x, 2000.

Quigley, M. C., Bennetts, L. G., Durance, P., Kuhnert, P. M., Lindsay, M. D., Pembleton, K. G., Roberts, M. E., and White, C. J.: The provision and utility of science and uncertainty to decision-makers: earth science case studies, Environment Systems and Decisions, 10.1007/s10669-019-09728-0, 2019.

Reichelt, R.: Géologie du Gourma (Afrique occidentale), un seuil et un bassin du Précambrien supérieur, Mém. BRGM, no 53, 1971.

Sanchez-Rojas, J., and Palma, M.: Crustal density structure in northwestern South America derived from analysis and 3-D modeling of gravity and seismicity data, Tectonophysics, 634, 97-115, https://doi.org/10.1016/j.tecto.2014.07.026, 2014.

Talwani, M., Worzel, J. I., and Landisman, M.: Rapid gravity computations for twodimensional bodies with application to the Mendicino submarine fracture zone, Journal of Geophysical Research, 64, 49-59, 1959.

Talwani, M., and Heirtzler, J. R.: Computation of magnetic anomalies caused by two-dimensional bodies of arbitrary shape, in: Computers in the Mineral Industries, edited by: Parks, G. A., School of Earth Sciences, Stanford University, 464-480, 1964.

Tarantola, A.: Popper, Bayes and the inverse problem, Nat Phys, 2, 492-494, 2006.

Telford, W. M., Geldart, L. P., and Sheriff, R. E.: Applied Geophysics, 2nd ed., Cambridge University Press, Cambridge, UK, 1990.

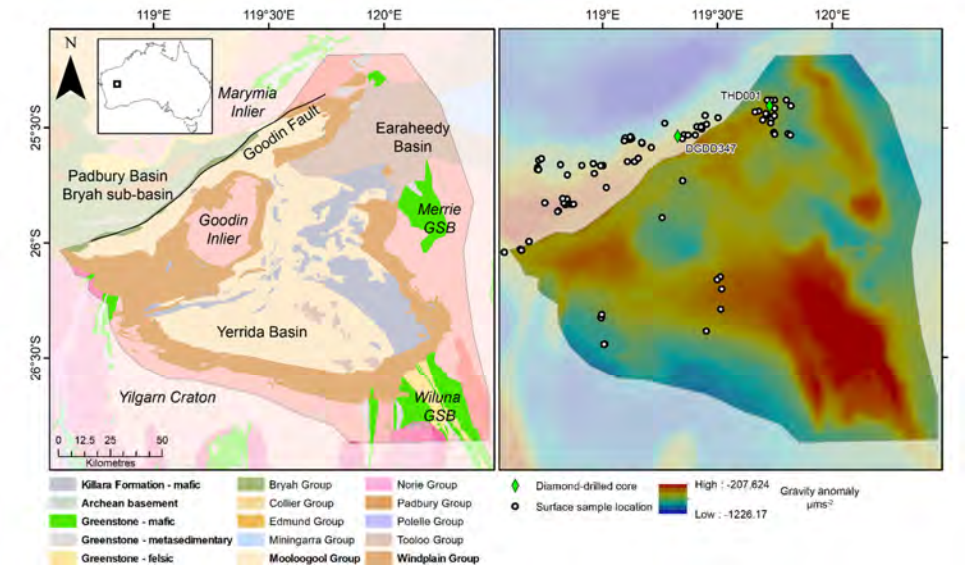

Figure 1. a) Location and geology of the Yerrida Basin, Capricorn Orogen ~~(left)~~. b) Bouguer gravity image of the Yerrida Basin shown with sampling locations for petrophysical and geochemical data. Points represent surface sample locations; diamonds represent location of diamond-drilled core collars with name. Significant regions are labelled, with Archean rocks shown with italic font. GSB = greenstone belt. The legend lists group-level stratigraphic units and those shown in bold are described in Figure 2. The shaded region indicates those outside the study area.

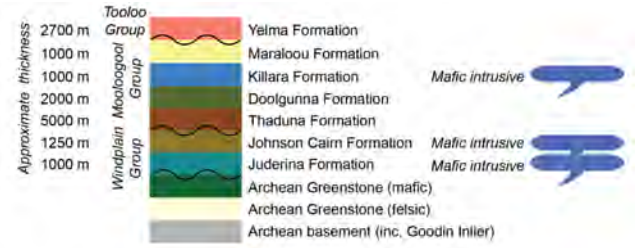

Figure 2. Stratigraphy and input for the Yerrida Basin 3D model modified from Occhipinti et al. (2017). The position of unconformities ~~are~~ is indicated with a wavy line and approximate thicknesses are given. The position of the mafic intrusives ~~are~~ is shown to indicate the possible stratigraphic position being tested by geophysical modelling. Unit colours correspond to those used in the 3D model (refer Section 4.6 3D Model and Figure 10).

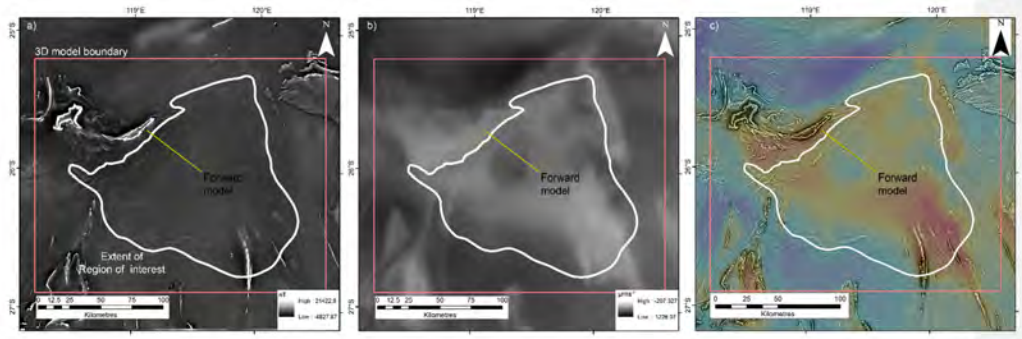

Figure 3. Geophysical grids and forward model location trace (as indicated). a) Magnetic anomaly, ~~and~~ b) Bouguer gravity anomaly and c) blended image of Bouguer anomaly (colour) and 1VD of the RTP magnetic data (greyscale).

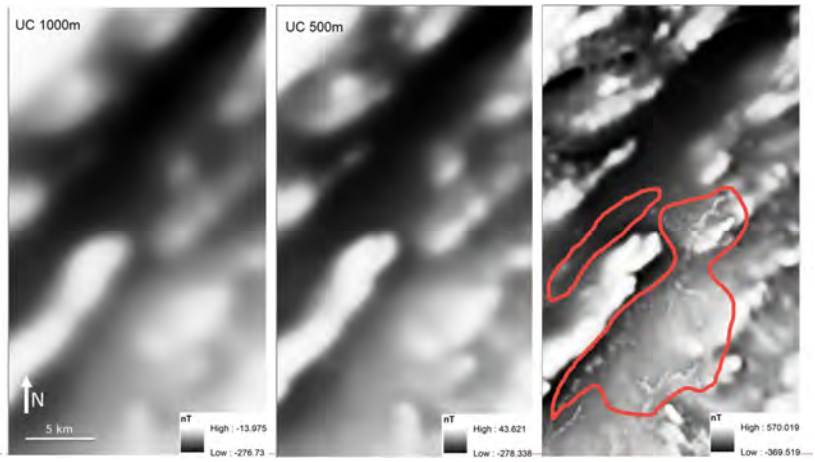

~~**Figure 4. In order to view non-regolith rock units, upward continuation was performed on RTP magnetic data to filter short wavelength magnetic anomalies attributed to surficial stream sediments and other forms of regolith. Upward continuation of 1000 m (left); 500 m (right) and the original, unfiltered RTP magnetic data. Examples of the types of anomaly that were targeted for filtering are circled in red. Such anomalies of surficial transported regolith add noise to a geophysical interpretation and increase the likelihood of misinterpretation of structure. Location is centred on 119.162 E – 25.908 S.**~~

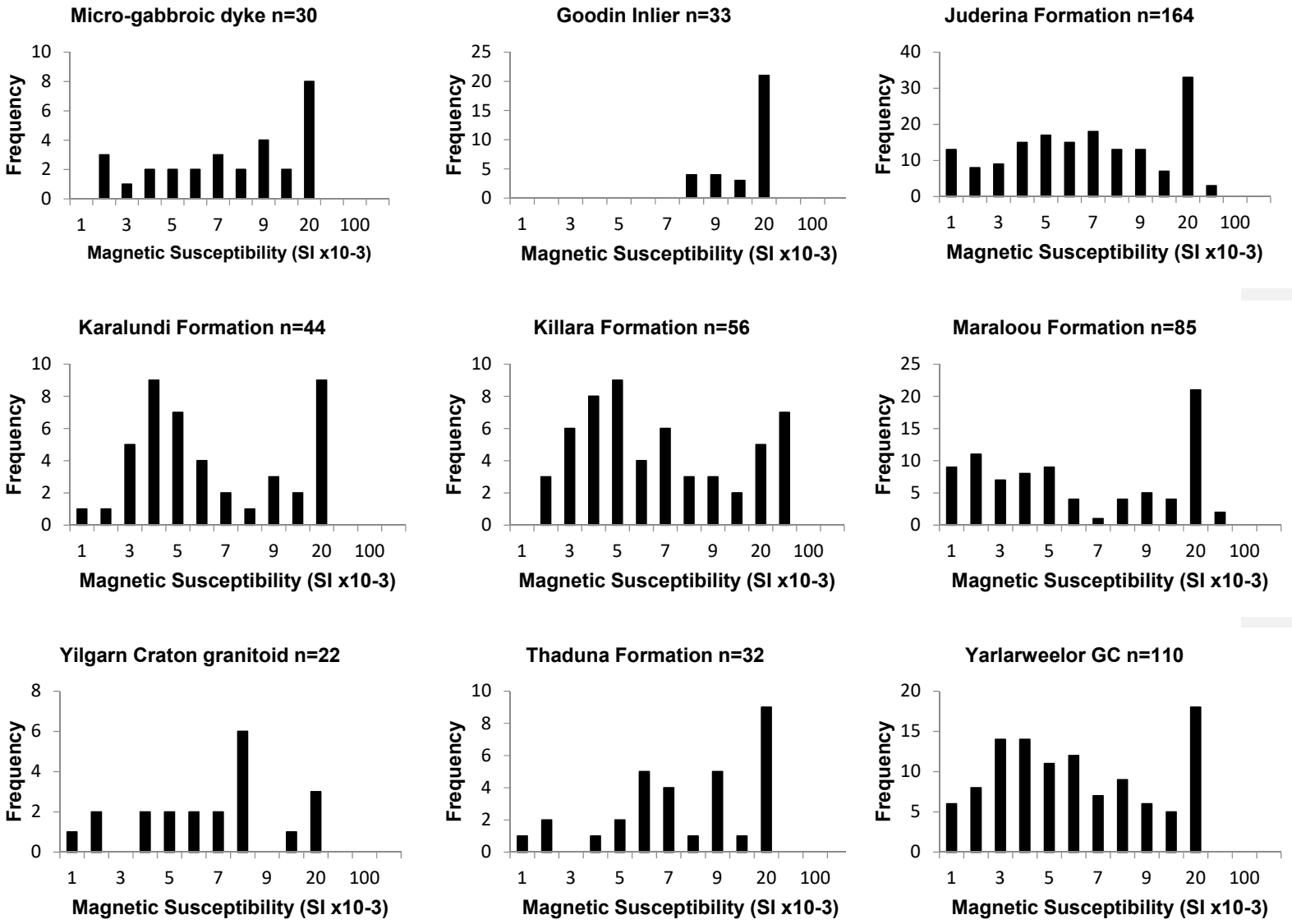

Figure 45. Histogram representation of measured magnetic susceptibility from Yerrida Basin rocks.

Field Code Changed

Formatted: Font: Bold

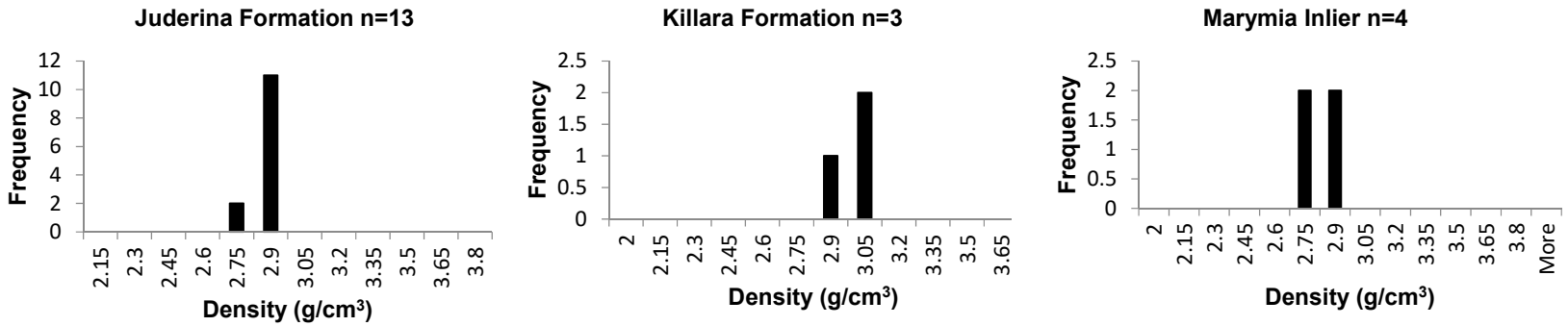

Figure 56. Histogram representation of measured Archimedes bulk density of Yerrida Basin rocks

Field Code Changed

Formatted: Font: Bold

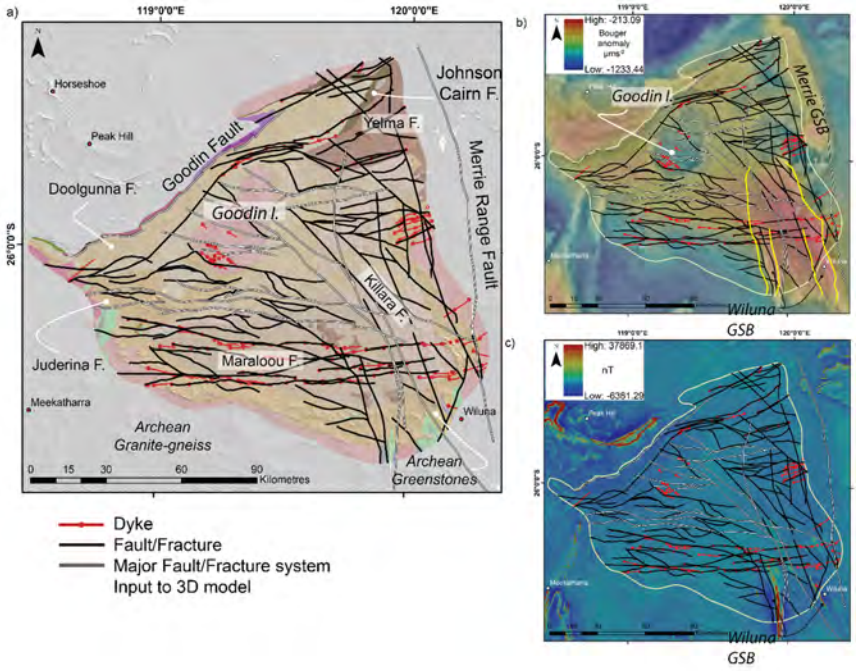

880 **Figure 67. Simplified Sstructural geophysical interpretation of the southern Yerrida Basin. (a) Integrated interpretation of structure and rock units with the highlighted major fault systems input to the 3D model (refer section 4.6 3D Model). The location of AEM line L1008802 is shown – refer Figure 8a. (b) Interpreted structure shown with gravity data (blended image: Bouguer anomaly shown in colour with 1VD of the Bouguer anomaly in greyscale). (c) Interpreted structure shown with blended magnetic data (blended image: RTP shown in colour with 1VD of the RTP shown in greyscale). GSB = greenstone belt.**

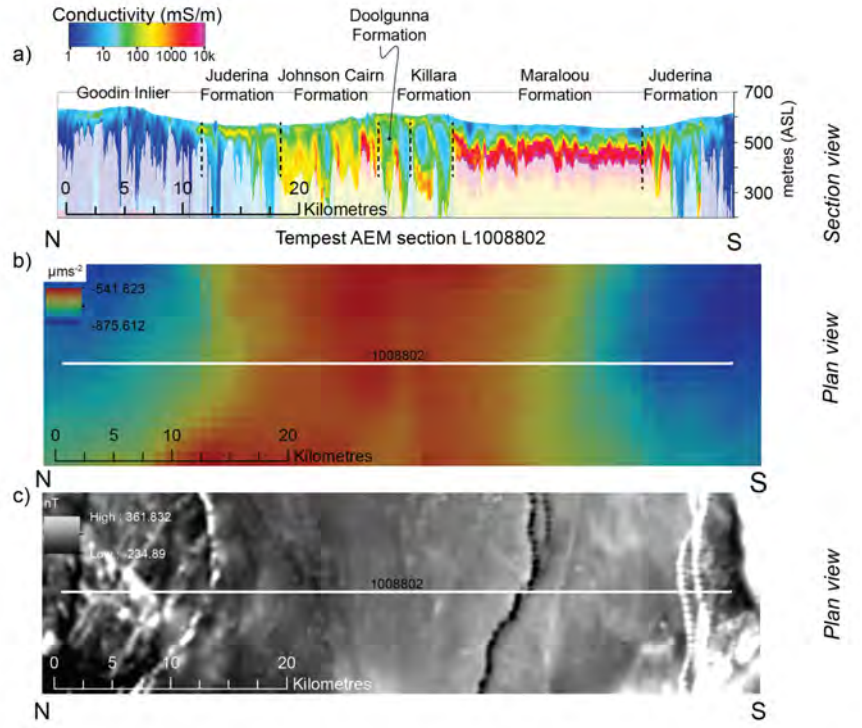

~~Figure 8. Airborne electromagnetic data (AEM) and lithological interpretation. AEM data was useful to distinguish lithologies to support the overall interpretation. a) Tempest AEM section L1008802 labelled with formations correlated to the surface geology maps (see Figure 7a for location). b) Plan view of the gravity grid at the same location. The lower resolution of this data proved less useful the AEM for lithological interpretation at this scale. c) Plan view of magnetic data at the same location. While higher resolution than the gravity data, lithological interpretation is more difficult compared to the imageing provide by AEM data.~~

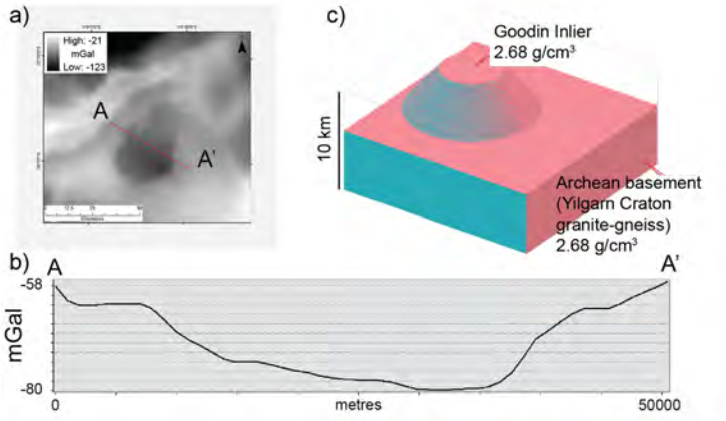

Figure 79. Initial conceptual model using 'Noddy': a) the observed gravity response from a part of the Yerrida Basin, showing the location of the profile in part b); b) curve representing the gravity response of the Goodin Inlier taken from the observed gravity; c) initial conceptual 3D model of the Goodin Inlier. The Yerrida Basin sedimentary rocks are modelled, but are not shown here for better visualisation of basement geometry.

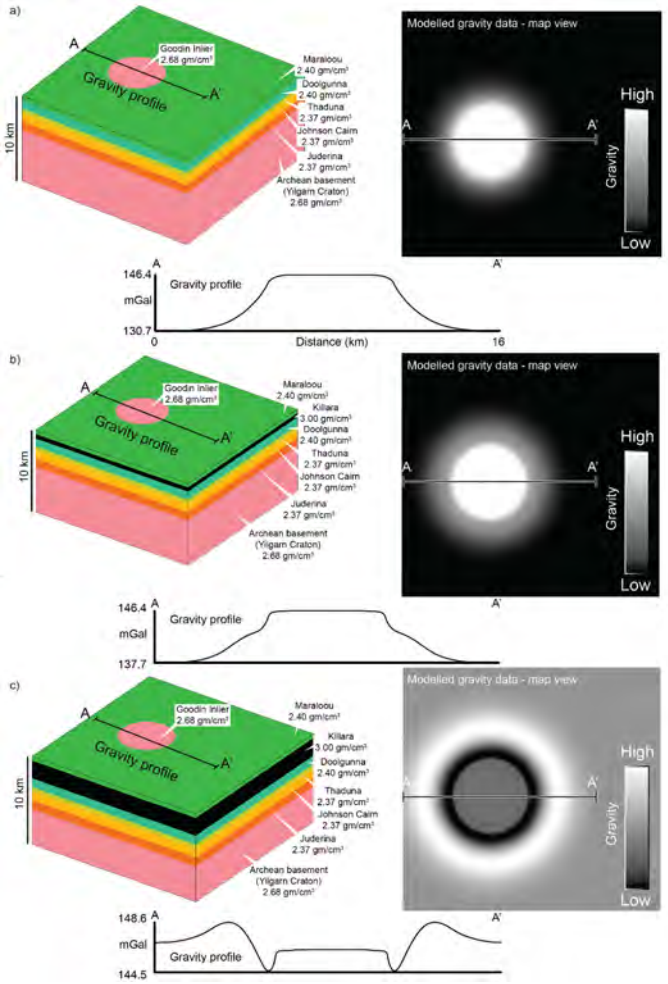

Figure 8~~10~~. Conceptual forward modelling results obtained from Noddy. (a) No Killara formation; (b) 500 m of Killara Formation and (c) 2000 m of Killara Formation.

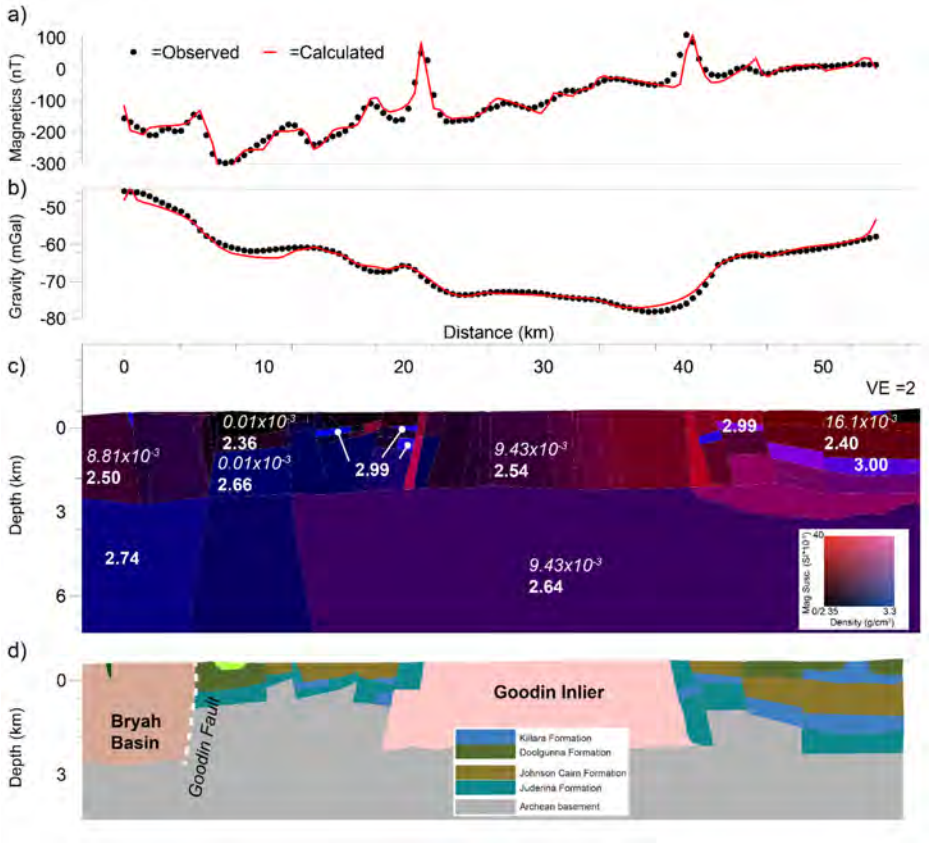

Figure 2~~11~~. Section-based forward modelling of the Yerrida Basin and Goodin Inlier – location of profile shown in Figure 2. The top two panels show the degree of fit between the observed (points) and calculated (line) geophysical response for magnetic (a) and gravity (b) data. The middle panel (c) shows the petrophysical model that was used to model the calculated geophysical response. Indicative petrophysical values are shown (bold: density – g/cm3; italics – susceptibility Six10-3) to help guide visualisation of the colour scale shown at right. The bottom panel (d) shows the geological interpretation made from the petrophysical model. Boundaries shown at the surface of the model are sourced from field observation and interpretation (refer section Table A 1).

Formatted: Centered

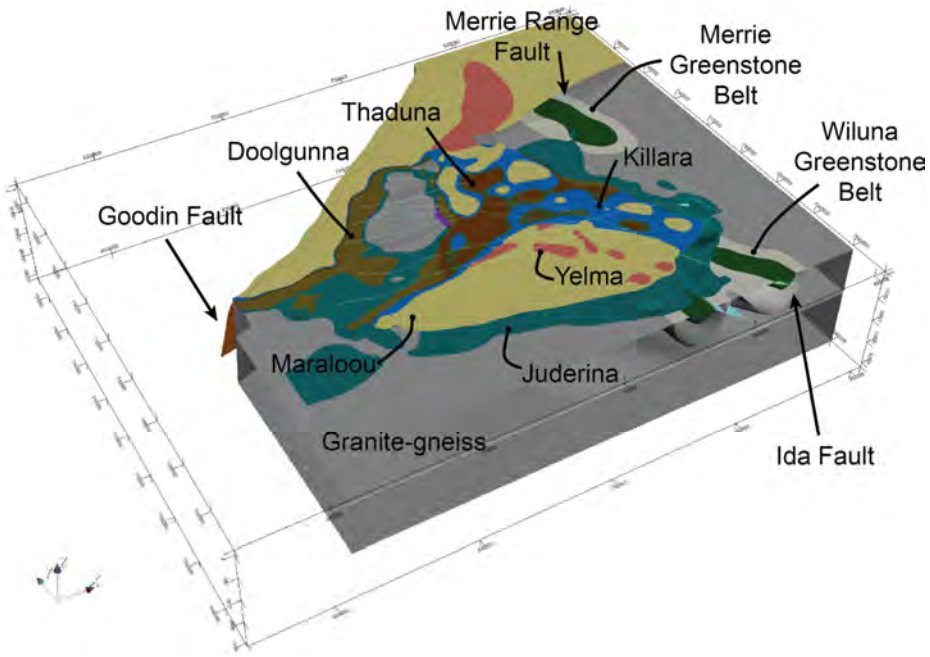

Figure 1012. 3D model constructed to constrain geophysical inversion. Oblique view from SW - check marks on the X-axis are at 50 km intervals; Y-axis at 20 km intervals; Z-axis 10 km.

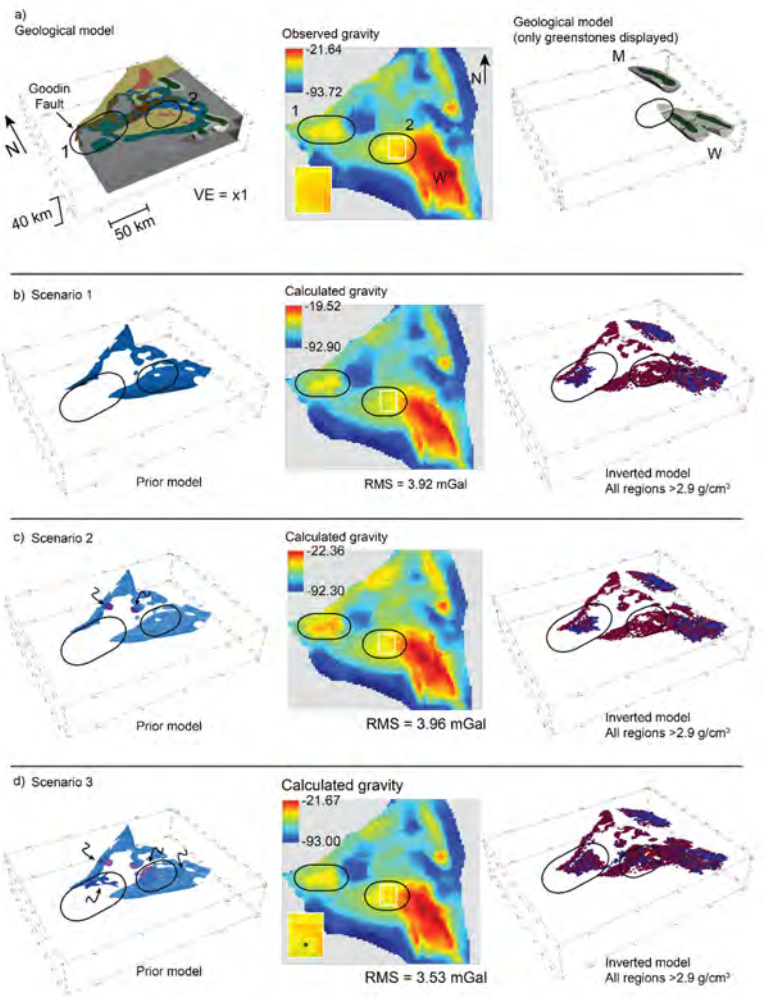

Figure 11~~13~~. Geological models and mafic intrusive scenarios subjected to inversion modelling. a) Top panel: 3D geological model (left); ~~middle panel –~~ observed gravity response (centre); ~~bottom panel –~~ location of greenstone belts (right). b-d) Results from scenarios 1-3 respectively: (left)~~top –~~ position of mafic intrusions; ~~middle –~~ calculated gravity response from inversion (centre); ~~bottom –~~ distribution of locations determined by the inversion to be >2.9 ~~g~~mg/cm3 (right). Scenario 2 and 3 incrementally introduce mafic bodies to the prior model (left-hand panes, c and d), as indicated by the arrows. Colours in the gravity response

Formatted: Centered

indicate blue = low; yellow = moderate; red = high. ~~Check marks on the X-axis are at 50 km intervals; Y-axis at 20 km intervals; Z-axis 10 km.~~

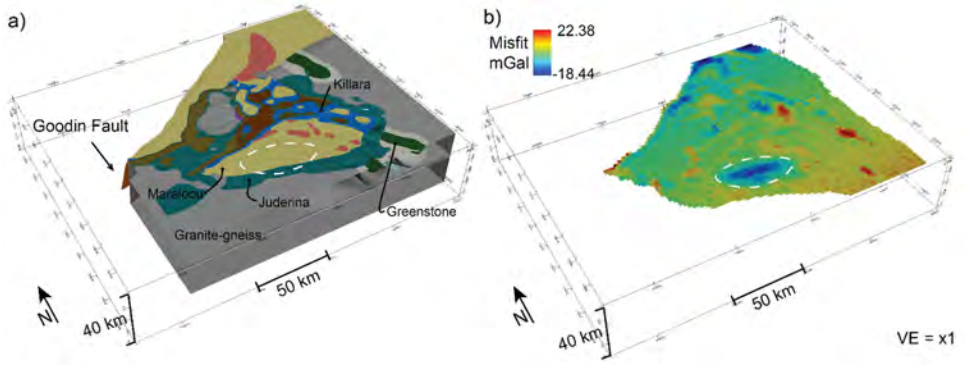

Figure 12~~14~~. Assessing the plausibility of the Yerrida Basin model with geological knowledge and geophysical inversion. a) The 3D model representing scenario 3 and b) the remaining misfit between the inverted geological model and geophysical data. Misfit values ~~is shown~~ after regional trend effects ~~have been~~were removed using a linear solver. Red = density exceeds that required by observed gravity, blue = density lower than that required by observed gravity. Note the large region of misfit outlined by the white dashed line that indicates the position of where a portion of high-density material needs to be ~~a~~removed ~~d~~ded to ~~result in~~ reduce~~d~~ misfit. The cause of this misfit is considered to be ~~due~~ in response to the modelled sedimentary basin rocks being too thick and not hosting the required volume of mafic material. ~~Check marks on the X-axis are at 50 km intervals; Y-axis at 20 km intervals; Z-axis 10 km.~~

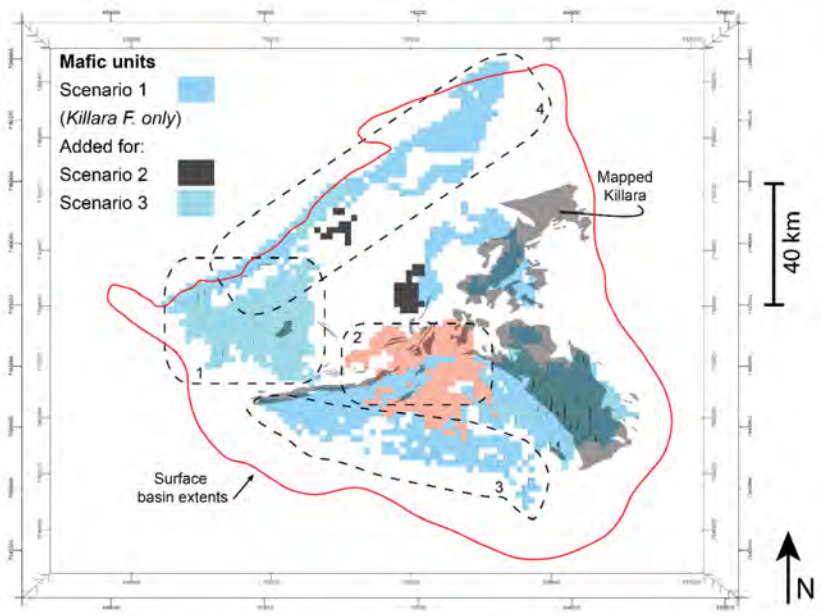

Figure 13~~15~~. Comparison of mafic units at depth with mapped Killara Formation. Mafic units are colour-coded to help differentiate bodies as added during scenarios 2 and 3 ~~testing~~. Check marks on the X-axis are at 50 km intervals; Y-axis at 20 km intervals; Z-axis 10 km.

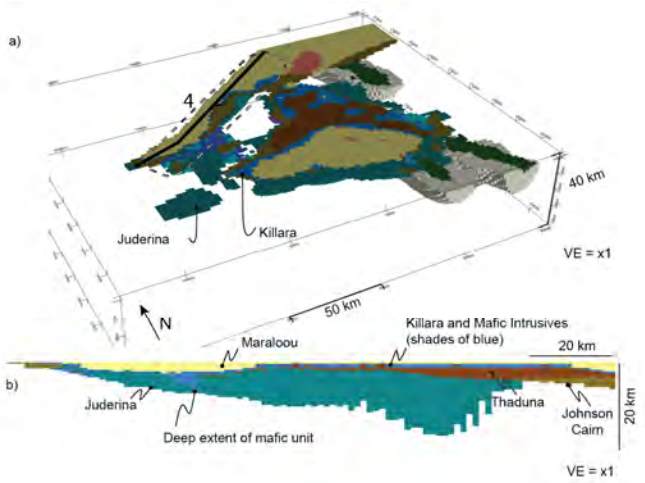
a)
4
Juderina
Killara
40 km
VE = x1
50 km
N
Killara and Mafic Intrusives
(shades of blue)
Maraloou
20 km
b)
Juderina
Deep extent of mafic unit
Thaduna
Johnson
Cairn
20 km
VE = x1

930

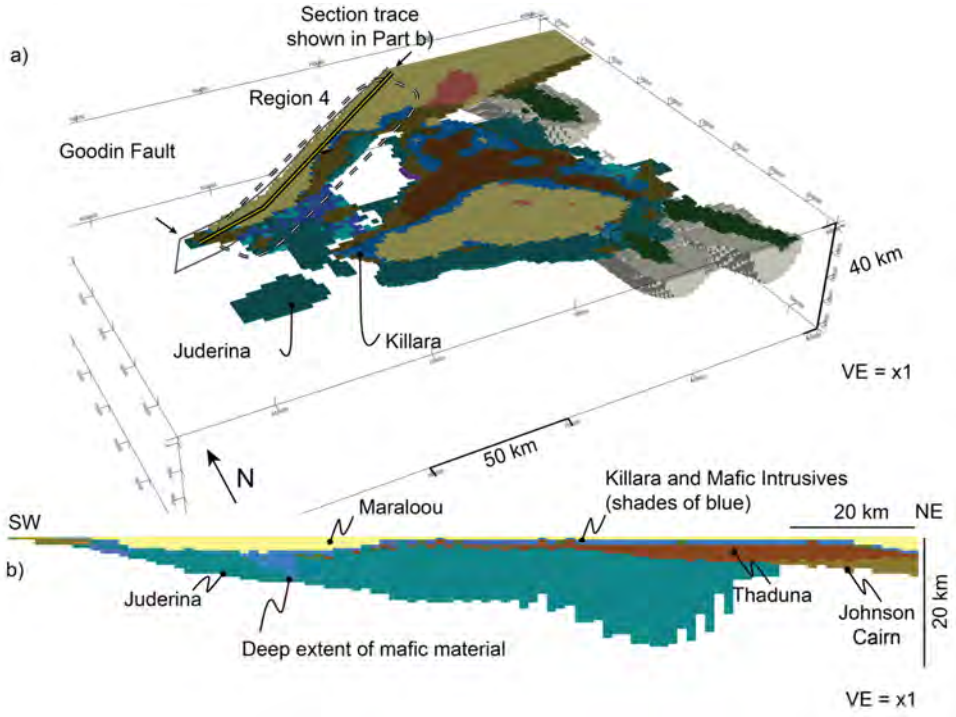

Figure 1416. 3D model ~~showing~~ and distribution of high–density (>2.9 ~~gm~~sg/cm3) mafic material around Region 4: a) Isometric ~~– d) show different views of the model, with regions discussed in-text labelled accordingly~~view of the inverted model from above and the southwest. The dashed line indicates Region 4 and the solid yellow and black line shows the location of the section. ~~Check marks on the X-axis are at 50 km intervals; Y-axis at 20 km intervals; Z-axis 10 km.~~ b) Section view of ~~trace show in a)~~Region 4 viewed from the southeast displaying the depth of the Juderina Formation and the deep extent of mafic material near the northwest extent of the Yerrida Basin.

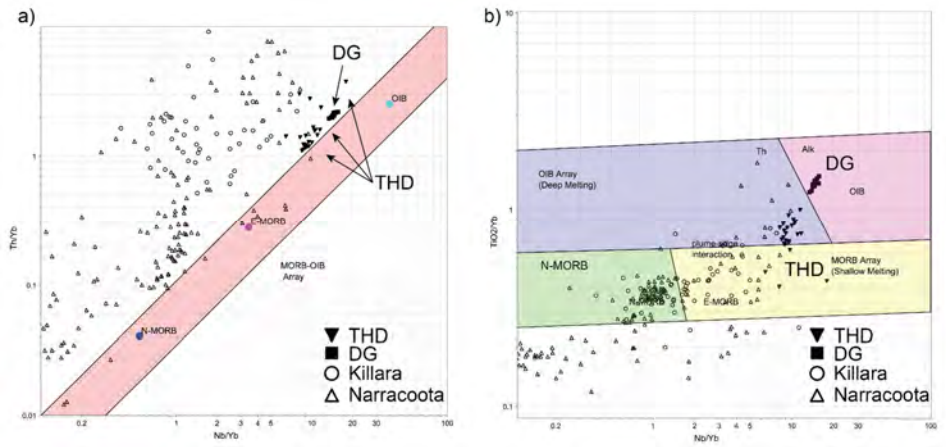

Figure 15~~17~~. a) Discriminant basalt Th/Yb vs Nb/Yb diagram of mafic geochemistry from the Yerrida Basin and b) discriminant Nb/Yb and TiO_2/Yb diagram. Data compiled from Olierook et al. (2018), DGDD347 and THD 001.

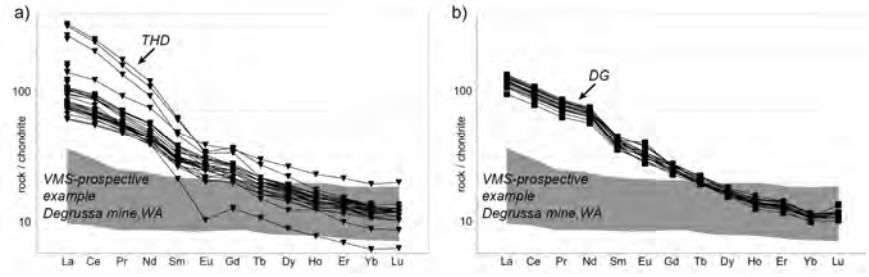

Figure 16~~18~~. REE spider diagrams for mafic rocks sampled from a) THD001 and b) ~~DDGD347~~DGDD347. Note the inclined profiles for each indicated a non-prospective environment for VMS mineralisation. The shaded portion indicates a VMS-prospective example taken from basaltic and micro-gabbroic rocks sampled from the Degrussa mine (Hawke, 2016).

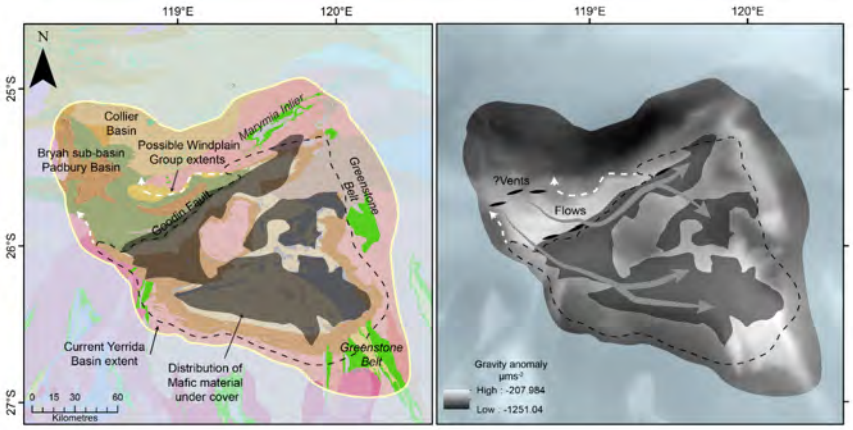

945

Figure 17~~19~~. Proposed source of magmatism for the mafic component of the Yerrida Basin. The lack of an Archean signature in the mafic rocks suggests that conduits for magmatism do not include the Yilgarn Craton rocks that underlie the Yerrida Basin, but likely sourced from the northwest or along the current position of the Goodin Fault. a) Major components of the southern Capricorn region are shown, with Archean regions listed in italics. Shaded regions show the position of mafic material determined via geophysical inversion. b) Vent locations and flow or sill intrusion paths are proposed and shown over the Bouguer gravity anomaly.

950

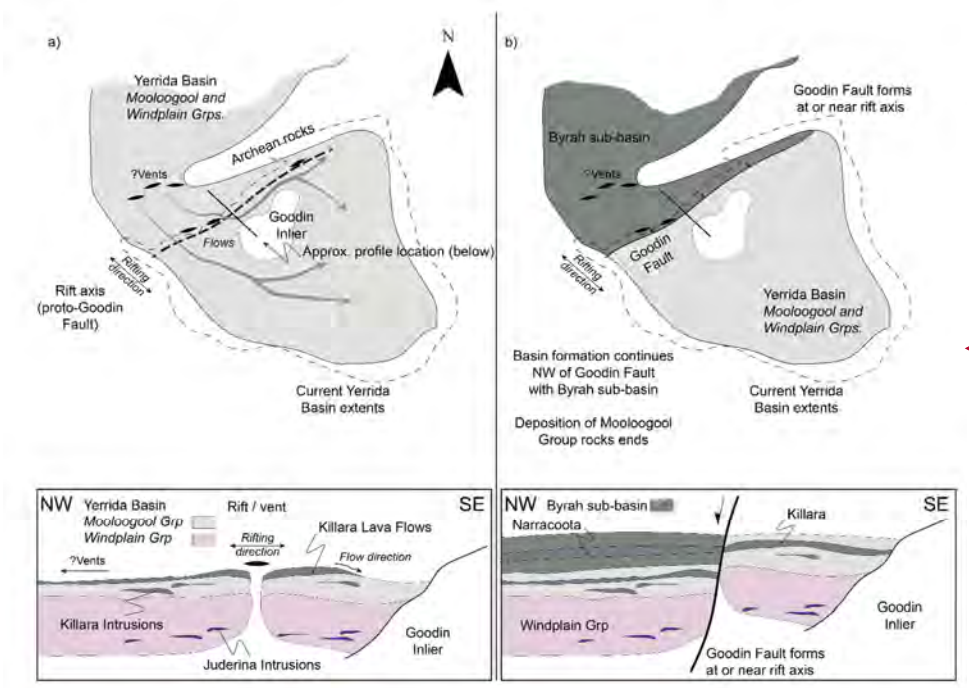

Figure 18. Schematic model for early development (c. 2200 Ma to c. 2000 Ma) of the Yerrida Basin showing map (top) and section views (below). a) Early deposition of Windplain and Mooloogool groups rocks under extension. A rift, which later becomes the Goodin Fault, is a hypothesised source of magmatism along with vents located to the northwest of the rift axis. This magmatism produces intrusions to the Juderina Formation. Flat paleotopography allows formation of intrusions and lava flows across, around and either side of the rift. The Killara Formation plausibly originates from these vents however sulphur isotope data is required to provide support for this hypothesis. b) Continued extension results in normal-faulting at or near the rift axis and emergence of the Goodin Fault. Deposition of the Bryah sub-basin is initiated to the northwest of the Goodin Fault. Magmatism continues at the vents in the northwest, producing the Narracoota Formation. The presence of the normal fault forms a barrier to Narracoota Formation lava flows flowing to and deposition of Bryah sub-basin rocks in the southeast.

Formatted: Normal

Table 1. Petrophysical statistics calculated from rock sample measurements.

Magnetic ~~Susceptibilty~~Susceptibility			
Formation / Rock type	*Sample size (n)*	*Mean ($SI \times 10^{-3}$)*	*Std. dev. ($SI \times 10^{-3}$)*
Dyke	30	6.20	4.26
Goodin Inlier	33	10.31	2.06
Juderina	164	5.04	4.16
Karalundi	44	5.14	2.62
Killara	56	5.74	6.16
Maraloou	85	4.76	3.83
Narracoota	127	3.36	2.58
Yilgarn Craton granitoid	22	5.54	3.63
Thaduna	32	6.66	5.19
Density			
		Mean (gm/cm^3)	*Std. dev. (gm/cm^3)*
Goodin Inlier	1	2.68	NA
Juderina	13	2.82	0.055
Killara	3	2.89	0.111
Marymia Inlier	4	2.73	0.086
Yilgarn Craton grantoid	2	2.68	0.029
Thaduna	1	2.40	NA